Atmospheric
Chemistry
and Physics
Discussions

Open Access

The impact of the chemical production of methyl nitrate from the NO + CH$_3$O$_2$ reaction on the global distributions of alkyl nitrates, nitrogen oxides and tropospheric ozone: a global modeling study

J. E. Williams[1], G. Le Bras[2], A. Kukui[3], H. Ziereis[4], and C. A. M. Brenninkmeijer[5]

[1]Royal Netherlands Meteorological Institute, De Bilt, the Netherlands
[2]Institut de Combustion, Aérothermique, Réactivité et Environnement, CNRS, Orléans, France
[3]Laboratoire de Physique et Chimie de lÉnvironnement et de lÉspace, CNRS, Orléans, France
[4]DLR, Oberpfaffenhofen, Germany
[5]Max Planck Institute for Chemistry, Atmospheric Chemistry, Mainz, Germany

Correspondence to: J. E. Williams (williams@knmi.nl)

Discussion Paper | Discussion Paper | Discussion Paper | Discussion Paper

ACPD
13, 20111–20163, 2013

The impact of the chemical production of methyl nitrate

J. E. Williams et al.

Title Page

Abstract   Introduction

Conclusions   References

Tables   Figures

|◄   ►|

◄   ►

Back   Close

Full Screen / Esc

Printer-friendly Version

Interactive Discussion

Full Screen / Esc

Printer-friendly Version

Interactive Discussion

Abstract

The formation, abundance and distribution of organic nitrates are relevant for determining the production efficiency and resident mixing ratios of tropospheric ozone (O_3) at both regional and global scales. Here we investigate the effect of applying the recently measured direct chemical production of methyl nitrate (CH_3ONO_2) during NO_x recycling involving the methyl-peroxy radical on the global tropospheric distribution of CH_3ONO_2 and the perturbations introduced towards tropospheric NO_x and O_3 using the TM5 global chemistry transport model. By comparing against numerous observations we show that the global surface distribution of CH_3ONO_2 can be largely explained by introducing the chemical production mechanism using a branching ratio of 0.3 %, when assuming a direct oceanic emission source of $\sim 0.29\,\mathrm{TgN\,yr^{-1}}$. The resident mixing ratios are found to be highly sensitive towards the dry deposition velocity of CH_3ONO_2 that is prescribed, where more than 50 % of the direct oceanic emission of CH_3ONO_2 is lost near the source regions thereby mitigating subsequent effects on tropospheric composition due to long range and convective transport. For the higher alkyl nitrates (C_2 and above) we find improvements in their simulated distribution in the tropics in TM5 improves when introducing direct oceanic emissions of $\sim 0.17\,\mathrm{TgN\,yr^{-1}}$. For the tropical upper troposphere (UT) a significant low model bias for all alkly nitrates occurs due to either missing transport pathways or chemical precursors, although measurements show significant variability in resident mixing ratios at high altitudes with respect to both latitude and longitude. For total reactive nitrogen (NO_y) ~ 20 % originates from alkyl nitrates in the tropical and extra-tropical UT, where the introduction of both direct oceanic emission sources and the chemical production of CH_3ONO_2 only increases NO_y by ~ 5 % when compared with aircraft observations. We find that the increases in tropospheric O_3 due to direct oceanic emissions are mitigated by introducing the direct chemical production of CH_3ONO_2 resulting in rather moderate effects on nitrogen oxides and tropospheric O_3.

1 Introduction

The chemical production of tropospheric ozone (O_3) is critically dependent on the recycling efficiency of NO to NO_2 involving peroxy-radicals (Atkinson et al., 2000). The most abundant peroxy-radicals in the troposphere are the hydro-peroxy (HO_2) and methyl-peroxy (CH_3O_2) radicals, which are predominantly formed during the photolysis of chemical precursors such as formaldehyde (HCHO) and the oxidation of methane (CH_4), respectively, as well as through the recycling of OH radicals. Once formed in Reactions (R1) to (R3) NO_2 is rapidly photolysed producing tropospheric O_3 by Reactions (R4) and (R5):

$$NO + HO_2 \rightarrow NO_2 + OH \tag{R1}$$

$$NO + CH_3O_2(+O_2) \rightarrow NO_2 + HCHO + HO_2 \tag{R2}$$

$$NO + RO_2 \rightarrow NO_2 + RO \tag{R3}$$

$$NO_2 + h\nu \rightarrow NO + O^3P \tag{R4}$$

$$O^3P + O_2 + M \rightarrow O_3 + M \tag{R5}$$
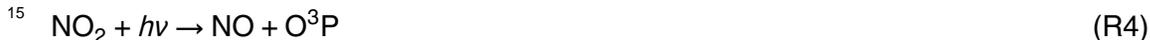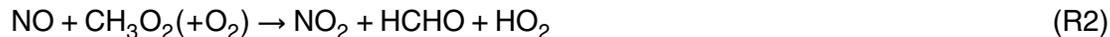
One competing reaction not directly involving peroxy-radicals is the regeneration of NO_2 via the titration of O_3, Reaction (R6), which is especially efficient in high NO_x environments exhibiting elevated mixing ratios of O_3.

$$NO + O_3 \rightarrow NO_2 + O_2 \tag{R6}$$

At global scale Reaction (R1) is the dominant NO_x recycling mechanism involving peroxy-radicals accounting for $\sim 65\%$ of total regeneration of NO_2, with Reactions (R2) and (R3) also being significant and accounting for $\sim 25\%$ and $\sim 10\%$, respectively (see

Title Page

Abstract | Introduction

Conclusions | References

Tables | Figures

|◄ | ►|

◄ | ►

Back | Close

Full Screen / Esc

Printer-friendly Version

Interactive Discussion

Sect. 6). Although Reaction (R6) is the major NO to NO_2 recycling mechanism, there is no net contribution towards the production of O_3 under steady state NO_x–O_3 conditions meaning that it acts as a moderating step.

The chain length of the free-radical reaction cycle described above is determined by the efficiency of the chain termination steps, mainly Reactions (R7)–(R9) below. These lead to the formation of long-lived nitrogen reservoirs: nitric acid (HNO_3), peroxy-acetyl nitrate (PAN) and organic nitrates (ORGNTR), respectively.

$$NO_2 + OH + M \rightarrow HNO_3 + M \tag{R7}$$

$$NO_2 + CH_3(O)O_2 + M \rightarrow PAN + M \tag{R8}$$

$$NO + RO_2 + M \rightarrow ORGNTR + M \tag{R9}$$

Although other termination reactions such as the self reaction of HO_2, the self reaction of RO_2 and the cross termination reaction of $HO_2 + RO_2$ maybe important under certain low NO_x conditions, for brevity we only list the dominant termination steps here. The competition between these terminating steps towards sequestrating reactive nitrogen is influenced by sources of Volatile Organic Compounds (VOCs), whose emissions act as chemical precursors of higher peroxy radicals (RO_2).

Although the individual steps of this reaction cycle have been studied extensively over the last decades there is still some uncertainty related to the possibility of long lived nitrogen reservoirs being formed directly during Reactions (R1) and (R2). For instance, recent laboratory measurements using chemical ionization mass spectroscopy have revealed formation of HNO_3 when investigating the product distribution from Reaction (R1), with the branching ratio being dependent on pressure, temperature and relative humidity (Butkovskaya et al., 2005, 2007). This has lead to a number of different global modelling studies associated with studying the impact of this branching ratio on tropospheric composition (Cariolle et al., 2009; Sovde et al., 2011; Gottschaldt et al., 2012; Boxe et al., 2012). The most important finding related to oxidative capacity

The impact of the chemical production of methyl nitrate

J. E. Williams et al.

Title Page

Abstract | Introduction

Conclusions | References

Tables | Figures

|◀ | ▶|

◀ | ▶

Back | Close

Full Screen / Esc

Printer-friendly Version

Interactive Discussion

is that significant reductions in the production of tropospheric O_3 were simulated due to a reduction in the recycling efficiency of NO, increasing the atmospheric lifetimes of dominant trace species such as CO and CH_4. However, some ambiguity still exists as to the catalytic effects of water vapour on the branching ratio (Butkovskaya et al.,
5 2009) meaning that the direct formation of HNO_3 is typically not included in chemical mechanisms employed in large-scale chemistry transport models (CTMs) nor currently included in the recommendations (e.g. Sander et al., 2011) due to the lack of an independent measurement for this branching ratio.

   Using the same technique Butkovskaya et al. (2012) recently detected the direct
10 formation of methyl nitrate (CH_3ONO_2) during a study of the products generated from Reaction (R2). The branching ratio (Reaction R10) inferred for tropospheric conditions is $1.0 \pm 0.7\%$ and has a weak temperature and pressure dependence:

$$NO + CH_3O_2 + M \rightarrow CH_3ONO_2 + M \qquad\qquad (R10)$$

Results from a recent conceptual modelling study by Farmer et al. (2011) have sug-
15 gested that the formation of organic nitrates during the conversion of NO to NO_2 by RO_2 under urban conditions has the potential to significantly reduce the photo-chemical production of O_3. Organic nitrates have also been found to be important for the lifetime of NO_x whenever the total NO_x mixing ratio is lower than 500 ppt (Browne and Cohen, 2012). Therefore, given the importance of Reaction (R2) in the remote tropical tropo-
20 sphere in terms of NO_x recycling due to efficient CH_4 oxidation (Fiore et al., 2006), the direct formation of CH_3ONO_2 can have implications for the global tropospheric O_3 burden and, thus, oxidative capacity. Another source of direct chemical production of CH_3ONO_2 which has been invoked in the past involves the decomposition of PAN, although this mechanism was later shown to be rather inefficient (Orlando et al., 1992)
25 and therefore not included in this study.

   Alkyl nitrates contribute significantly to the total reactive nitrogen (NO_y) budget of the troposphere (e.g. Buhr et al., 1990) but their measurement remains difficult. Nonetheless they have been measured under a wide range of atmospheric conditions (e.g.

The impact of the chemical production of methyl nitrate

J. E. Williams et al.

|◄ | ►|

◄ | ►

Back | Close

Full Screen / Esc

Printer-friendly Version

Interactive Discussion

Flocke et al., 1998a,b; Roberts et al., 1998; Swanson et al., 2003; Jones et al., 2011). In Tables 1a and b we provide an overview of mixing ratios of CH_3ONO_2 which have been measured at both the surface and in the Free Troposphere (FT, between 2–10 km), respectively, where values are grouped in latitudinal zones. Although a large fraction of alkyl nitrates are formed in the gas phase via Reaction (R9), other direct sources of alkyl nitrates are thought to exist from direct oceanic emissions (Atlas et al., 1993; Chuck et al., 2002; Dahl et al., 2005) and, to a lesser extent, biomass and savannah burning (Simpson et al., 2002). Measurements of resident mixing ratios made over the tropical ocean, along with concentration gradients of dissolved organic nitrates measured in seawater surface, infer aqueous phase production till super-saturation occurs, followed by a release into the Marine Boundary Layer (MBL), with a dependency on the dissolved nitrite concentrations (Dahl et al., 2008). Such oceanic emissions act as a direct source of additional nitrogen reservoirs into low NO_x environments without the need of long range transport. This biogenic source is likely to exhibit a latitudinal gradient related to the temperature of the surface waters and biological activity (Chuck et al., 2002; Dahl et al., 2007). For instance, measurements made at coastal sites in the US have found that direct emission from the ocean waters only makes a minor contribution to resident mixing ratios of CH_3ONO_2 near the East coast (Russo et al., 2010). Measurements on the Antarctic around 70–75° S have revealed that surprisingly high resident mixing ratios of between 2–14 ppt of CH_3ONO_2 exist, indicating a possible link to NO_x emissions from snow (e.g. Weller et al., 2002; Wang et al., 2007), where CH_3ONO_2 is the most abundant of the alkyl nitrates at these southerly latitudes (Jones et al., 2011). Similar measurements at the South Pole show a maximum of C_1-C_3 alkyl nitrates during Austral wintertime (Beyersdorf et al., 2010) who propose the source not to be direct emissions from the snowpack but rather transport from oceanic regions implying oceanic emissions. Therefore the actual source of CH_3ONO_2 at these southerly latitudes is still the subject of some debate.

To investigate the global impacts on atmospheric composition, Neu et al. (2008) have used a CTM including the direct emission of alkyl nitrates from oceanic sources and

shown that they exert an impact on the tropospheric O_3 and NO_x budgets in the tropics. In their study they adopted apriori emission estimates based on the measurements presented in Blake et al. (2003a) for both CH_3ONO_2 and ethyl nitrate ($C_2H_5ONO_2$). However, the chemical formation of CH_3ONO_2 via Reaction (R10) was not considered. Including Reaction (R10) could go some way to accounting for the observed resident mixing ratios in the remote marine troposphere (e.g. Blake et al., 2003a), on Antarctica and in the FT (Walega et al., 1992; Flocke et al., 1998). This would result in a lower emission flux estimate being needed to explain ambient air measurements. Once present, alkyl nitrates are removed by either deposition processes (e.g. Russo et al., 2010), direct photolytic dissociation or oxidation by OH (Talukdar et al., 1997a,b) to release NO_2. Thus the potential reduction in the production efficiency of tropospheric O_3 by Reaction (R2) due to the sequestration of reactive nitrogen in Reaction (R10) has the potential to neutralize the effects due to increased oceanic nitrogen emissions.

In this paper we investigate the global impact that the proposed chemical formation of CH_3ONO_2 has on composition of the global troposphere by using the tropospheric version of the global 3-D Chemistry Transport Model (CTM) TM5. In Sect. 2 we provide a description of the version of TM5 used for the study, the emission estimates adopted for precursor trace gases and the updates made compared to previous versions and details of the inclusion of CH_3ONO_2. In Sect. 3 we examine the distribution of both CH_3ONO_2 and higher alkyl nitrates in TM5 after including both the direct oceanic emission sources and the chemical production from Reaction (R10). In Sect. 4 we compare the distribution of alkyl nitrates at high latitudes and in the tropics against those measured during a number of intensive campaigns and we identify the sensitivity of the vertical and regional distribution towards assumptions in both emissions and chemical formation. In Sect. 5 we examine how the introduction of extra nitrogen into the troposphere alters the reactive nitrogen budget and also identify the impact of chemical formation of CH_3ONO_2. In Sect. 6 we show the effects on tropospheric NO_x, O_3 and OH and discuss implications for the atmospheric lifetimes of greenhouse gases. Finally in Sect. 7 we present our conclusions.

2 Model description

2.1 The TM5 model

In this study we use the 3-D global CTM TM5 (Huijnen et al., 2010; Williams et al., 2012) which employs the modified CB05 chemical scheme. This mechanism has recently been comprehensively described and validated in Williams et al. (2013) so for brevity we do not provide many details here. We perform simulations at a horizontal resolution of $3° \times 2°$ and use 34 vertical levels from the surface up to ~ 0.5 hPa. TM5 is driven using meteorological fields taken from the ERA-interim re-analysis (Dee et al., 2011), using an update frequency of 3 h. The details of which parameters from the meteorological fields are used in TM5 are given in Huijnen et al. (2010). The chosen simulation year is 2008 and all simulations use 2007 as a one year spin-up period to reach chemical equilibrium.

Some modifications which improve TM5 compared to previous versions have also been incorporated (e.g. Williams et al., 2013) as described here. As this version of TM5 only contains tropospheric chemistry observational constraints are applied in the stratosphere for species such as CH_4 and O_3 (Huijnen et al., 2010) are used. We also adopt new boundary conditions for HNO_3 based on the HNO_3 / O_3 ratios derived using latitudinal climatologies assembled from measurements by the ODIN instrument between 2001 and 2009 (Jégou et al., 2008; Urban et al., 2009), where instantaneous forcing is applied at 10 hPa. This provides a more realistic seasonal evolution of HNO_3 in the stratosphere when compared to that simulated when using the UARS climatology as performed in previous versions (Huijnen et al., 2010; Williams et al., 2012), especially in the Polar regions. Previous studies have shown that the global dry deposition flux of carbon monoxide (CO) in TM5 was rather high accounting for the loss of 160–180 Tg CO yr^{-1} (e.g. Williams et al., 2012). In this study the loss of CO at the surface by enzymatic processes in the soil (Yonemura et al., 2000) is parameterized with respect to the soil moisture content according to Sanderson et al. (2003). The resistive fluxes are then passed into the dry deposition scheme of Ganzeveld and Lelieveld (1995).

This reduces the global dry deposition flux by around $\sim 80\,\mathrm{Tg\,CO\,yr^{-1}}$. Further updates associated with dry deposition include increasing the surface resistance for CO over oceans and of O_3 over snow and ice.

For this study we have included CH_3ONO_2 explicitly as an additional transported tracer species into the modified CB05 chemical mechanism described by Williams et al. (2013). The atmospheric lifetime of CH_3ONO_2 is estimated to range from around a week to a month depending on atmospheric conditions (Talukdar et al., 1997a,b), meaning that it can be transported out of the Boundary Layer (BL, the first few kilometres near the surface) into the FT and beyond. This is compared to atmospheric lifetimes of between several days to weeks for the C_2-C5 alkyl nitrates (Clemitshaw et al., 1997). Both the photolytic destruction and oxidation of CH_3ONO_2 by OH are included using the chemical reaction data taken from Talukdar et al. (1997a,b) forming the products NO_2 and HCHO. We also include a dry deposition term equal to that used for the higher alkyl nitrates (ORGNTR) for the majority of the simulations. A small wet deposition term is also included using the values of Kames and Schurath (1992).

2.2 Definition of the emission scenarios and sensitivity studies

The emission estimates used here are described Williams et al. (2013) thus only briefly summarised here. For anthropogenic emissions we use a hybrid complied using the RETRO inventory (Schultz et al., 2007; http://retro.enes.org) and the REAS inventory for the Asian region (Ohara et al., 2007) between 60–150° E and 10° S–50° N. The exception is for CH_4 which we take from EDGARv4.2 (http://edgar.jrc.ec.europa.eu/). For biomass burning emissions we use the GFEDv3 monthly emission inventory (van der Werf et al., 2010). For biogenic emissions we use the estimates provided by MEGANv2 (Guenther et al., 2006) except for CH_4 which we take from the LPJ-WhyMe inventory (Spahni et al., 2011). For lightning NO_x we use the parameterization of Meijer et al. (2001). The CH_4 distribution in the boundary layer is constrained by nudging

Title Page

Abstract | Introduction

Conclusions | References

Tables | Figures

◀ | ▶

◀ | ▶

Back | Close

Full Screen / Esc

Printer-friendly Version

Interactive Discussion

to a seasonally dependant latitudinal gradient using the method given in Williams et al. (2013).

In total six sensitivity studies are defined and listed in Table 2. In addition to the BASE simulation, which does not explicitly include CH_3ONO_2, these are namely: (i) EMISS which applies a direct apriori oceanic emission for CH_3ONO_2 of $26.7\,\mathrm{mg\,m^{-2}\,s^{-1}}$ ($\sim 0.29\,\mathrm{Tg\,yr^{-1}}$) as taken from Neu et al. (2008) and applied between 10° S–10° N (ii) DEMISS which applies a direct apriori oceanic emission flux for CH_3ONO_2 twice that of EMISS to represent an upper limit (iii) LOWBR where we adopt a low branching ratio of 0.3 % for the chemical formation of CH_3ONO_2 (the lower limit of the experimental data in Butkovskaya et al., 2012), (iv) HIGHBR with a branching ratio of 1.0 %, (v) EMISSPT where we reduce the direct emission by 50 % compared to EMISS and apply the low branching ratio of 0.3 %, (vi) EMISSDD as EMISSPT except we double the dry deposition flux of CH_3ONO_2 and (vii) FLIGHT as EMISSPT except we use a branching ratio of 0.045 % which is the mean value suggested by Flocke et al. (2008) derived from measurements in the Upper Troposphere (UT, above 10 km till the tropopause). In the EMISS, EMISSPT, EMISSDD and FLIGHT simulations we also include the direct emissions of ORGNTR from the ocean adopting an estimate of $15.62\,\mathrm{mg\,m^{-2}\,s^{-1}}$ ($\sim 0.17\,\mathrm{Tg\,N\,yr^{-1}}$) which is twice the apriori estimate calculated for $C_2H_5ONO_2$ in Neu et al. (2008) so as to represent the release of other alkyl nitrates such as e.g. isopropyl nitrate as measured over the tropical ocean (Dahl et al., 2005). Direct emissions of organic nitrates from the oceans are applied out away from coastlines by using the land-sea mask threshold of 15 % in each grid cell to exclude large freshwater lakes and land locked bodies of water in the tropics. In our study no oceanic emissions are applied in the SH like in the Neu et al. (2008) as motivated by the measurements of Blake et al. (2003a). The emission of alkyl nitrates from the ocean has been linked to both the concentration of chlorophyll and sea temperature (Chuck et al., 2002; Dahl et al., 2008). A strong seasonality exists in the chlorophyll concentrations in the SH (Myriokefalitakis et al., 2010) resulting in maximal concentrations occurring during the boreal wintertime, therefore any resulting emission flux is likely to exhibit a similar sea-

The impact of the chemical production of methyl nitrate

J. E. Williams et al.

Title Page

Abstract	Introduction
Conclusions	References
Tables	Figures

⏮ ⏭

◀ ▶

Back | Close

Full Screen / Esc

Printer-friendly Version

Interactive Discussion

sonality. The small emission of CH_3ONO_2 measured from biomass and savannah fires ($\sim 18\,Gg\,yr^{-1}$, Simpson et al., 2002) is an order of magnitude lower than the ocean emission flux and thus not included in this study.

2.3 Observational datasets

To investigate to what degree TM5 is able to capture a realistic global distribution of alkyl nitrates at global scale we compare co-located model output against independent measurements made at selected stations and by research aircraft. Relevant details on these sites and campaigns are given below.

The Halley Bay research station at coastal Antarctica (75.3° S, 26.4° W) is situated 32 m a.s.l. and located on the Brunt Ice shelf. It is surrounded on three sides by the Wedell Sea and can be near ice-free water during the austral summer months. For our study we use the measurements presented in Jones et al. (2011) taken as part of the Chemistry of the Antarctic Boundary Layer and the Interface with Snow (CHABLIS) campaign which took place from February 2004 to January 2005. Measurements were determined from flasks which were stored, transported and analysed in the UK by Gas Chromatography–Mass Spectroscopy.

Neumayer in Antarctica (70.0° S, 8.2° W) is a well established measurement station. It is located on an ice-shelf ~ 10 km away from the Northeast Weddell Sea, and is considered to be representative of a location with pristine air transported either over the snow pack on Antarctica or from over the surrounding Ocean and sea ice. Here we use the measurement values published by Weller et al. (2002) who analysed air from flasks by gas chromatography to determine mixing ratios of alkyl nitrates.

The Mauna Loa Observatory is located at ~ 3.4 km a.s.l. in Hawaii (19.5° N, 155.6° W) situated in the remote northern Pacific Ocean. It has a long standing history of measuring atmospheric composition, where we use values observed during the Mauna Loa Observatory Photochemistry Experiment (MLOPEX, Ridley and Robinson, 1992). These measurements are representative of FT air and therefore should provide information regarding background mixing ratios. Again, the measured values published

in Walega et al. (1992) are derived using gas chromatography with a detection limit of ~ 0.3 ppt for organic nitrates.

For the extra-tropical NH we use the values provided in Roberts et al. (1998) measured at Cherbogue Point, Nova Scotia (43.8° N, 66.1° W) as part of the North Atlantic Regional Experiment (NARE; Fehsenfeld et al., 1996) during August and September of 1993. The measurement site is located at the tip of a peninsular about 10 km south of Yarmouth, Nova Scotia. The location was chosen such that strong anthropogenic NO_x sources towards the south did not impinge significantly on the measurements, although there was some local ship traffic (Fehsenfeld et al., 1996). Therefore measurements are thought to be representative of the remote conditions affected by oceanic air masses.

To assess the vertical distribution of CH_3ONO_2 and higher alkyl nitrates in the TM5 model in the tropics we use data measured during a number of different flights conducted as part of the second Pacific Exploratory Mission (PEM-tropics B; Raper et al., 2001) between March and April 1999 in the region 76° E–148° W and 36° S–38° N. Measurement data from both the DC-8 and P-3B aircraft have been used, which use different instrumentation for measuring the mixing ratios. For the comparison we interpolate 3 hly model data to the altitude and location at where the measurements were taken. The measurement data are averaged approximately every minute to avoid fluctuations in mixing ratios due to small scale variability. These measurements have been presented in Blake et al. (2003a) and provide valuable information regarding the tropospheric distribution of these important NO_x reservoirs.

Finally, we use chemical NO_y measurements from the second phase of the Civil Aircraft for Regular Investigation of the Atmosphere Based on an Instrument Container (CARIBIC) project which started in 2005 and is running up to the present date (Brenninkmeijer et al., 2007). In this instance NO_y is defined as the cumulative sum of all reactive nitrogen species, namely NO, NO_2, PAN, HNO_3, HNO_4, N_2O_5 and all alkyl nitrates. All trace constituents are reduced to NO during the measurement meaning that no values are available for individual reservoir species. We use in-situ measurements made from April till December 2008 made on flights which travelled from Frankfurt,

Germany (50.0° N, 8.5° E) to Chennai, India (13.0° N, 80.2° E). The flights to and from Chennai take similar routes providing a monthly snapshot of the distribution of NO_y at the cruise altitude of 10–12 km throughout a large fraction of the year. The uncertainty associated with the CARIBIC NO_y measurements is $\sim 8\%$ for mixing ratios around 450 ppt. We only use measurements which are representative of the upper troposphere (UT) restricting us to the latitude range 15–30° N.

3 The annual mean distribution of CH_3ONO_2 and ORGNTR

Figure 1 shows both the annual zonal and horizontal mean distributions of CH_3ONO_2 for EMISS, along with the corresponding absolute differences in mixing ratios relative to EMISSPT given in ppt, thus differentiating the impact of Reaction (R10). For the annual horizontal mean distribution mixing ratios are averaged between the surface and 800 hPa so as to give a representative mean of the first few kilometres of the troposphere. The total cumulative emission of CH_3ONO_2 in EMISS is equivalent to $\sim 0.3\,Tg\,N\,yr^{-1}$ and results in a global tropospheric burden of 0.015 Tg N. The highest mixing ratios of between 40–60 ppt occur in the tropical MBL directly above the emission sources, where CH_3ONO_2 is lifted out of the MBL reaching the UT. Long range transport towards higher latitudes then occurs by the large-scale atmospheric circulation. Unlike the vertical distribution shown in Neu et al. (2008), which exhibits maximal mixing ratios both in the BL and higher up in the UT, we do not get any increases in mixing ratios above 10 km in EMISS but rather a continuous decrease as determined by the increasing efficiency of photolytic destruction with altitude and that the only source in EMISS is emission at the surface. We also do not have high mixing ratios in the SH as we only introduce oceanic emissions in the tropics. There appears to be a large variability in the vertical profile of CH_3ONO_2 from the available measurements when comparing campaigns. For instance the measurements of Flocke et al. (1998a) indicate that the mixing ratio of CH_3ONO_2 should be between 1–3 ppt around 11 km at tropical latitudes almost matching the zonal mean values shown for EMISS. However,

the profiles shown in Blake et al. (2003a) show higher mixing ratios in the tropical UT of between 10–15 ppt. This is possibly related to a significant longitudinal variability in emission sources. Without the chemical production of CH_3ONO_2 from a chemical precursor any profile should have a negative gradient if photolytically active in the tro-

5　posphere. The long range transport of CH_3ONO_2 out of the tropics below 800 hPa at higher latitudes is shown to be negligible. The global tropospheric lifetime of CH_3ONO_2 in EMISS is $\sim$ 31 days, at the high end of the estimates of between 7 days to a month (Butkovskaya et al., 2012). Destruction predominantly occurs in the tropics, where dry deposition accounts for $\sim$ 80 % of the total sink term. However, in these simulations

10　we did not employ a specific deposition flux for CH_3ONO_2 but use that of higher alkyl nitrates as a proxy, which is assumed to be equal to that of PAN (Huijnen et al., 2010). This sink value is probably too low because CH_3ONO_2 has a higher solubility than other higher alkyl nitrates (Russo et al., 2010). We discuss another simulation where the deposition velocity of CH_3ONO_2 is increased later on (cf. Table 2).

15　　When introducing Reaction (R10) absolute differences in CH_3ONO_2 mixing ratios of between 40–80 ppt occur. The largest increases occur over continental regions in the NH around the sub-tropics and tropics in the FT where most NO_x is emitted. It should be noted that these increases occur in spite of the direct oceanic emission term of CH_3ONO_2 being decreased by 50 % between simulations to account for the introduc-

20　tion of a mixed source (see Table 2), resulting in the direct emission of CH_3ONO_2 be-ing equivalent to $\sim$ 0.13 Tg N yr^{-1} in EMISSPT. This is smaller than the total CH_3ONO_2 formed in Reaction (R10), where a discussion regarding the annually integrated chem-ical budget terms is provided later on in Sect. 5. Examining the corresponding changes in the distribution of the CH_3O_2 radical (not shown) in EMISSPT reveals that increases

25　of $\sim$ 5–10 % in the resident mixing ratios occur in both the BL and FT around the equator, showing a positive feedback of Reaction (R10) with respect to CH_4 oxida-tion (see Sect. 6 for further discussion on oxidative capacity). This enhanced yield of CH_3ONO_2 is somewhat moderated by the associated decrease in NO (not shown) from the enhanced sequestration of nitrogen to CH_3ONO_2. The global tropospheric burden

of CH_3ONO_2 increases significantly to 0.08 Tg N (~ five times that found in EMISS). This increases the resulting global lifetime to 42 days, again with dry deposition being the dominant loss term (~ 76 %). When performing a similar comparison with HIGHBR (not shown) increases in the CH_3ONO_2 mixing ratios of hundreds of ppt occur through-
5 out the troposphere, which is too high when compared with available measurements (see Sect. 4). For this reason the HIGHBR is not further considered.

    When analysing the horizontal distribution in the absolute changes in the mixing ratios it follows that the highest differences are situated in the NH between 10–30° N over North Africa, the Middle East and India. Part of this variability can be related to the
10 regional differences in the deposition terms for CH_3ONO_2 as shown in Fig. 2. Here the regional variability in annual deposition terms from EMISSPT is given, where the integrated annual deposition varies by an order of magnitude depending on surface type. The highest annual deposition occurs over the tropical oceans near regions close to where direct oceanic emissions are prescribed. The lowest deposition occurs over arid
15 regions such as the Sahara and Antarctica. Examining the chemical budget terms for EMISS (Sect. 5) shows that half of the CH_3ONO_2 released from tropical emissions is lost by local deposition. This rapid turnover highlights the importance of placing constraints on deposition velocities by measurements, especially over the ocean whose surface area in the tropics exceeds that of the continents. Such information would help
20 the modelling community in being able to gauge the ability of atmospheric models towards capturing this important physical sink process.

    Figure 3 shows the corresponding global distribution of ORGNTR in the BASE simulation. In the modified CB05 mechanism ORGNTR is predominantly formed via the conversion of NO with the NO_x operator species XO_2N (Gery et al., 1989 and Sect. 5)
25 and the oxidation of isoprene with the nitrate radical. It can be seen that the highest mixing ratios occur in regions where both anthropogenic and biogenic emissions dominate (e.g. East Asia and over Amazonia). Analysing the annual zonal mean shows that in the FT mixing ratios are higher in the NH. When examining the absolute differences in ORGNTR between BASE and EMISS reveals the highest increases in resident mix-

The impact of the chemical production of methyl nitrate

J. E. Williams et al.

ing ratios occur directly over the emission source regions. In our simulations we double the emission flux used in Neu et al. (2008) so as to be representative of a number of different C_2–C_4 alkyl nitrates that have been measured in the tropical Marine Boundary Layer (MBL), which typically have individual mixing ratios of between 3–6 ppt (Dahl et al., 2005). This results in $\sim 0.17\,\mathrm{Tg\,N\,yr^{-1}}$ being emitted directly into the remote tropical MBL, where analysing the differences shows that there is $\sim 100\,\%$ increase in resident mixing ratios. The global tropospheric burden in the EMISS simulation is 0.93 Tg N giving a global tropospheric lifetime of 30.1 days, which is comparable to the estimates given in the literature (Clemitshaw et al., 1997).

4   Comparisons against surface and aircraft measurements

Over the last few decades there have been a number of measurement campaigns and initiatives that have observed CH_3ONO_2 mixing ratios at pristine locations providing some information regarding background mixing ratios found in the troposphere. In Table 1a and b we have summarised the resident mean mixing ratios of CH_3ONO_2 available in the literature as observed over the last few decades showing the vertical and latitudinal variability which exists at global scale. For our purpose we subsequently select some of the surface sites and the also measurements of Blake et al. (2003a, b) to validate the global distribution of CH_3ONO_2 simulated in TM5.

Figure 4 shows the daily variability in CH_3ONO_2 for DEMISS, HIGHBR, EMISSPT and EMISSDD at Cherborge point, Nova Scotia (44° N, 66° W), Mauna Loa, Hawaii (20° N, 156° W) and Neumayer (70° S, 8° W) and Halley (75° S, 26° W) stations in Antarctica. We exclude EMISS as the transport to the measurement sites is negligible and therefore cannot explain the observed mixing ratios. For these comparisons 3 hourly model output is averaged into daily means to partially account for the impact of any diurnal cycle on resident mixing ratios due to photolytic destruction. The measurement data derived at these sites have been published in Roberts et al. (1998), Walagu et al. (1992), Weller et al. (2002) and Jones et al. (2011), respectively, where

measurements are shown in Fig. 4 whenever the scale allows. The comparison clearly shows that HIGHBR results in an excess of CH_3ONO_2, with mixing ratios approximately an order of magnitude too high at the NH sites shown and a factor of 2 too high on Antarctica. Assuming that there is not an important sink process missing from the simulations, these comparisons suggest that the lower limit of the branching ratio measured by Butkovskaya et al. (2012) seems the most plausible value provided.

At Cherborge Point (where a mean value of ∼ 2 ppt has been observed in the summertime) DEMISS provides the best agreement with mixing ratios of between 2–5 ppt solely due to the long range transport of CH_3ONO_2 from the tropics. However, at a measurement site on the East Coast of the US more southerly than Cherborge Point, Russo et al. (2010) found that higher CH_3ONO_2 measurements correlated with continental air masses influenced by anthropogenic emissions and therefore could not be explained by oceanic sources. In these simulations EMISSPT, which accounts for the chemical production of CH_3ONO_2 in polluted air masses, overestimates observed mixing ratios by an order of magnitude implying the need for either a larger sink term via dry deposition (Russo et al., 2010) or lower regional NO_x emissions from e.g. soil. Although the correlation with the observations is moderately better for EMISSDD than EMISSPT we still employ a dry deposition term with the ratio against O_3 of ∼ 0.6 compared with unity as suggested in Russo et al. (2010) based on observations. However deposition velocities are related to the type of terrain as shown in Fig. 2 meaning measurements at local scale cannot typically be adopted across wide areas showing the necessity for more measurements of deposition fluxes of alkyl nitrates at diverse locations.

At Mauna Loa (having a mean value of 3.6 ± 1.8 ppt throughout May; Walega et al., 1992) the air is sampled in the remote FT and thus dominated by the long range transport of CH_3ONO_2 from other source regions as shown for other trace species by Jaffe et al. (1997) during spring. An example of this in our simulations is the increase in CH_3ONO_2 which can be seen around day 180 in both HIGHBR and EMISSPT but not DEMISS, where DEMISS shows a signature of northerly transport from the tropics. DEMISS overestimates mixing ratios by around 5–10 ppt, with EMISSPT enhancing

this overestimation suggesting the atmospheric lifetime of CH_3ONO_2 is too long what-ever the source. Conversely, EMISSDD underestimates observed mixing ratios again, showing the sensitivity of the comparisons to the prescribed emission and deposition fluxes.

At Neumayer and Halley (with mean values of 8–10 ppt and 6–14 ppt, respec-tively) EMISSPT catures realistic mixing ratios compared with the measurements, with EMISSDD being much too low. Comparing DEMISS shows that the transport of CH_3ONO_2 to the high latitudes of the SH becomes visible during the Austral winter when no photolytic destruction occurs. This variability in photolysic activity imposes a seasonal cycle in the model simulations, with mixing ratios of CH_3ONO_2 during the austral wintertime being approximately double those during the austral summertime due to the longer lifetime. One missing potential source of NO_x in this study is the emission of NO from the snowpack, which has been found to affect the local nitro-gen reservoirs in the gas phase such as HNO_3 (Wang et al., 2007). However, mixing ratios of CH_3O_2 are of the order of a few ppt at the high latitudes therefore, consid-ering the low branching ratio, this would only act as a minor additional source during austral summer. In the study of Neu et al. (2008) mixing ratios of between 35–40 ppt of CH_3ONO_2 are shown in the BL for latitudes below 60° S as a result of prescribing emissions in the SH. These are too high when compared to the measurements (see Table 1a and b), similar to HIGHBR. Previous studies have shown that the observed variability in CH_3ONO_2 at Neumayer does not show any correlation with the origin of air masses suggesting a rather ubiquitous or local source (Weller et al., 2002). Looking at the lack of any significant seasonal cycle in EMISSPT shows that long range transport of CH_3ONO_2 from other regions contributes a dominant fraction to the simulated rather than local chemical production. Unfortunately there are no measurements available at these measurement sites over the months July and August to show whether higher mixing ratios of CH_3ONO_2 occur during Austral summertime.

Next we compare the tropical distribution of CH_3ONO_2 and ORGNTR in TM5 with those observed in the measurement data from the PEM-tropics B campaign during

March 1999. The PEM-tropics B data is scaled up 2.13 times as instructed by the data providers (D. Blake, personal communication, 2013). The routes of the flights which are used in this study are presented in Fig. 5, with flights from the DC-8 and P-3B being shown as separate colours. It can be seen that measurements taken over a wide area are used for our comparison. Although our simulation is for 2008 rather than 1999, the emissions employed are not dependent on wind speed, chlorophyll distributions or sea-surface temperature. However, the transport in the troposphere could be affected by inter-annual variability in the wind fields rather than e.g. precipitation fields, with wet deposition of CH_3ONO_2 via precipitation being a minor loss route. Given the weak temperature and pressure dependence of Reaction (R10) the chemical production term should also not be influenced to any significant extent. The measurement data is binned at a resolution of 100 m altitude in order to aid interpretation of the comparisons. The variability in the measurements can be significant in any one altitude bin (not shown) as measurements used for any particular altitude bin are sampled over a wide range of longitudes as shown in Fig. 5.

Figure 6 shows the comparisons of five different simulations against measured CH_3ONO_2 distributions using data which is sorted between the latitudinal limits of 10–20° N, 10° S–10° N and 10–20° S. Data taken from both of the aircraft involved in the campaign are shown on the same comparison, although the number of measurements in each latitudinal bin is not equal, where less weight should be put on the northern comparisons (see Fig. 5). Interpolated model output from EMISS, DEMISS, LOWBR, EMISSPT and EMISSDD is compared directly against the measurements. The measurements show that the vertical distribution in CH_3ONO_2 exhibits the steepest gradient in the tropics (10° S–10° N) implying a stronger oceanic emission source than the other latitudinal regions thus agreeing with the other independent observations (Dahl et al., 2005). For the other latitudinal regions the vertical gradient is either rather shallow (NH) or appears concave (SH) implying that long range transport plays a significant role between 9–10 km.

The distribution of CH_3ONO_2 in EMISS and DEMISS at 10–20° S and 10–20° N shows the extent of transport out of the tropics during March. Although the model profiles look quite similar in both latitudinal bands, the differences in the vertical distribution of CH_3ONO_2 in the the measurements result in neither simulation being able
5 to capture the correct distribution throughout. Focussing on the SH, EMISS appears low whereas DEMISS captures the distribution more accurately in the FT. Significant overestimations can be seen for LOWBR and EMISSPT, although mixing ratios in the MBL agree quite well unlike in EMISS and DEMISS. In part this is due to the application of strict latitudinal constraints on where the emissions occur. To improve on this
10 future studies could exploit chlorophyll maps from satellites such as MODIS as demonstrated by Myriokefalitakis et al. (2010) for marine organic aerosol formation. However, our study is more focussed on the influence of the chemical production term therefore such a step is beyond the scope of this study.

Analysing the comparison in the tropics shows that DEMISS captures the observed
15 gradient rather well, especially the range of values observed in the MBL. Comparing EMISS shows that the emission flux calculated by Neu et al. (2008) leads to underpredictions throughout the tropopsheric column. For FLIGHT (not shown), which adopts the branching ratio derived in Flocke et al. (1998a) (i.e. 4.5×10^{-3}) the contribution due to chemical production is far too small to improve on EMISS. The contribution from Re-
20 action (R10) is shown in LOWBR, demonstrating the importance of chemical production in the UT as concluded by Flocke et al. (1998a), albeit at a more efficient rate. Although Reaction (R10) improves the comparison in the FT, the low model bias persists across simulations. Given that the atmospheric lifetime of CH_3ONO_2 is rather long compared to literature estimates further implies that the mixing ratios in the UT are heavily influ-
25 enced by long range transport into thr tropics, which is currently missing in the model. An improvement on LOWBR occurs in the MBL when adding an emission term as in EMISSDD showing that a mixture of direct emissions and chemical production provides the optimal comparison, although again affected by the prescribed deposition velocity.

The impact of the chemical production of methyl nitrate

J. E. Williams et al.

Title Page

Abstract | Introduction

Conclusions | References

Tables | Figures

|◄ | ►|

◄ | ►

Back | Close

Full Screen / Esc

Printer-friendly Version

Interactive Discussion

To provide some assessment as to the ability of TM5 towards capturing the correct vertical distribution of ORGNTR, Figure 7 shows the corresponding comparison against combined measurement data for BASE and EMISS. Here the measurement data represents the sum of different higher alkyl nitrates, namely: $C_2H_5ONO_2$, i-$C_3H_7ONO_2$, n-$C_3H_7ONO_2$ and 2-$C_4H_9ONO_2$. For discussion regarding the chemical production of ORGNTR in TM5 the reader is referred to Sect. 5. As for CH_3ONO_2, the introduction of oceanic emissions of ORGNTR has little effect away from the source region but improves the quality of the comparison in the tropics between $10°$ S–$10°$ N up to ~ 5 km. Again a significant fraction is lost to the surface (see discussion on global chemical budgets in next section) and, again, there is a low model bias in the UT again due to a missing contribution due to long range transport. Although chemical production mechanisms for the higher alkyl nitrates have been measured involving higher peroxyradicals, they are thought to be more relevant in polluted plumes due to high VOC mixing ratios (e.g. Butkovskaya et al., 2010) and NO_x. The horizontal resolution of the simulations does not allow chemical processes in plumes to be captured potentially leading to an underprediction from the anthropogenic emissions. One other influence could be that in TM5 the photolysis rate for ORGNTR is calculated using the absorption characteristics of 2-$C_4H_9ONO_2$ due to the lack of experimental data for the other higher alkyl nitrates (Williams et al., 2012), although the effects on the atmospheric lifetime are unknown.

Finally, Fig. 8 shows comparisons of co-located model output with chemical measurements taken at ~ 250 hPa in the northern tropics and sub-tropics at selected latitudes from the CARIBIC observatory. We use measurements taken over most of the year during 2008. Although no direct measurements of alkyl nitrates are available from CARIBIC due to the measurement technique employed these measurements do allow an assessment of the impact of Reaction (R10) on the seasonal variability of NO_y near the tropopause, unlike the other measurements which are typically limited to a few months of the year. The measurement data is binned using $2°$ latitudinal intervals, with both the outward and return flight data used for the CARIBIC averages which are

shown. The 1-σ deviation from the observed mean is also shown (dashed lines) which quantifies the variability in the measurement data. We compare directly against BASE , DEMISS and EMISSPT. Examining the seasonal trend in the observations shows that between 15–25° N there is a maximum in NO_y mixing ratios during springtime, which generally decreases by $\sim$ 30–50 % towards December. Previous studies have shown that emissions directly below the flight path have an impact on composition of the UT over India (Schuck et al., 2010). This reduction in NO_y through the year maybe partially explained by the occurrence of the Indian Monsoon, where a larger fraction of NO_y is lost via wet deposition, but also by the change in the location of the tropopause. To a large degree TM5 manages to capture the seasonal variability in NO_y, although the total NO_y is typically too low across all selected latitudes by $\sim$ 10–30 %. To investigate what fraction of the modelled NO_y is due to total alkyl nitrates we show comparisons of BASE where the mixing ratios of these trace constituents are omitted. It can be seen that they contribute $\sim$ 20 % of the total model NO_y, therefore being less important than either HNO_3 or PAN.

The fractional increase in UT NO_y in DEMISS is limited to a few percent even at latitudes nearer the source region. From the PEM-tropics data comparisons shown in Figs. 5 and 6 it can be concluded that the model underestimates CH_3ONO_2 in the UT across the tropics, although the contribution of the missing alkyl nitrates towards the missing NO_y is constrained to less than 100 ppt thus not sufficient to entirely account for the underestimation of NO_y in TM5. Comparing DEMISS and EMISSPT shows that including Reaction (R10) only makes a marginal contribution to the observed seasonal dependence in the UT. For EMISSDD and FLIGHT (not shown) there is little difference from DEMISS. One reason for the low bias in the model is the impact of stratospheric intrusions which contain substantial mixing ratios of HNO_3 which the model fails to capture even with the new constraints applied from the ODIN instrument. This can be potentially improved by constraining lower down in the stratosphere rather than restricting the fixing application of constraints at 10Hpa. In summary, accounting for

the direct emission and chemical formation of alkyl nitrates improves the distribution of NO_y in the UT in TM5.

5 The influence on global annual chemical budgets of alkyl nitrates

In this section we decompose the global chemical budget terms of selected simulations
from Table 2 to examine whether the increase in tropospheric O_3 formation due to the
direct oceanic emissions of CH_3ONO_2 (Neu et al., 2008) is mitigated by the enhanced
sequestration of reactive nitrogen via Reaction (R10). Table 3 provides the global tropospheric chemical budget terms for CH_3ONO_2 as derived from EMISS, DEMISS, EMISSPT, EMISSDD and FLIGHT, respectively. Here we define the troposphere as
the 150 ppb contour as described in Stevenson et al. (2006). Analysing EMISS shows
that an additional $\sim 0.3\,\mathrm{Tg\,N\,yr^{-1}}$ is introduced into the troposphere when adopting the
apriori emission estimates. However, only $\sim 47\,\%$ (equivalent to $\sim 0.13\,\mathrm{Tg\,N\,yr^{-1}}$) is oxidised with the rest being lost by deposition to the surface. For the fraction oxidised,
photolytic destruction accounts for $> 90\,\%$ of the total loss term, although this maybe
too high as concluded from the comparisons shown in Fig. 5. The similar fractional loss
for DEMISS shows that this result seems to scale rather linearly with the oceanic emission flux term. Therefore, the impact of the direct oceanic emissions is much lower than
for other NO_x sources such as lightning NO_x or aircraft emissions in the FT, where surface deposition does not act as a major loss route. Analysing EMISSDD shows Reaction (R10) converts $\sim 1.0\,\mathrm{Tg\,N\,yr^{-1}}$ of reactive nitrogen in the form of NO into CH_3ONO_2
during 2008. This exceeds the additional N released by direct oceanic emissions. The
subsequent increase in the dry deposition term results in a net loss of $\sim 0.5\,\mathrm{Tg\,N\,yr^{-1}}$
from the troposphere as CH_3ONO_2. Thus Reaction (R10) significantly reduces the impact on tropospheric O_3 formation from the direct oceanic emissions (see Sect. 6) by
enhancing the loss of nitrogen to the surface (see below). Comparing the budget terms
for the EMISS and FLIGHT simulations provides further evidence that introducing Re-

action (R10), albeit with a very low branching ratio, enhances the dry deposition of CH_3ONO_2 by $\sim 58\%$.

Table 4 provides the corresponding tropospheric budget terms for the higher alkyl nitrates in the form of ORGNTR. Here we limit the comparison to between the BASE and EMISSDD simulations, with Reaction (R10) being negligible for the ORGNTR budget (see below). At global scale, ORGNTR is formed from reactions involving NO and the NO_x operator species XO_2N (Gery et al., 1989) or oxidation involving the nitrate radical (from night-time chemistry). As for CH_3ONO_2 chemical formation dominates that arising from oceanic emissions ($14.5\,TgN\,yr^{-1}$ compared to $0.2\,TgN\,yr^{-1}$). Once converted into ORGNTR only $\sim 40\%$ of NO_x is regenerated by photolysis or oxidation by OH. Thus $\sim 9\,TgN\,yr^{-1}$ of the total globally emitted nitrogen is lost by deposition to the surface when adopting the current emission estimates. Comparing both production and destruction terms for ORGNTR between BASE and EMISSDD shows they are approximately equal meaning Reaction (R10) introduces no significant feedback. The resulting global burden of ORGNTR increases by a few percent. We also show the total summed N deposition terms for NO_2, HNO_3, PAN and ORGNTR. Here N deposition increases by $\sim 0.15\,TgN\,yr^{-1}$ (also for EMISS, not shown) thus ultimately the additional N introduced by direct emission is almost entirely lost via deposition.

6 The Impact on global oxidative capacity

Finally in this section we examine the impact of Reaction (R10) on the distribution of tropospheric NO_x, O_3 and the subsequent changes towards the oxidizing capacity of the troposphere via perturbations in OH. In TM5, the transported tracer species NO_x represents the sum of short-lived nitrogen radicals and radical reservoirs namely NO, NO_2, NO_3, HNO_4 and N_2O_5. Table 5 provides the annual global production efficiency of O_3 by NO_x recycling due to Reactions (R1), (R2) and (R8) for BASE, EMISS, EMISSPT and EMISSDD, along with deposition totals and the global tropospheric burdens of O_3. In Figs. 9a–c we show the global annual mean distribution of NO_x, O_3 and OH

in the LT for BASE, respectively. Also shown are the relative percentage differences between BASE, EMISS and EMISSDD as integrated in the lower few kilometres of the atmosphere (below $\sim 800\,hPa$) for 2008.

Figure 9a shows that the highest annual mean mixing ratios of NO_x occur near regions which have high anthropogenic activity, including visible signatures along shipping tracks. For the remote tropical MBL NO_x mixing ratios are of the order 0–50 ppt, where Roberts et al. (2012) have shown that alkyl nitrates play an important role towards tropospheric O_3 formation under such chemical regimes. In EMISS an increase in NO_x mixing ratios of up to $\sim 10\,\%$ occurs around the emission sources. The limited transport and efficient deposition of CH_3ONO_2 in the BL mean that for the subtropics and extra-tropics effects are limited to around $\pm\ 0.2\,\%$. For EMISSDD, decreases in NO_x mixing ratios of between 0–5 % occur at all latitudes with the exception of the tropical Pacific where the emissions are the highest and thus dominate over the sequestration of additional nitrogen. A more marked effect is seen in the SH away from direct NO_x sources, where the termination steps (6) to (8) are less efficient due to lower radical mixing ratios.

Figure 9b shows that the largest increases in tropospheric O_3 of between ~ 1–5 % are located around the tropics (20° S–20° N) in EMISS directly near the oceanic sources (see Figs. 1 and 3). Here O_3 mixing ratios in TM5 are of the order of 20–30 ppb. For the other latitudinal zones there is a more muted increase in tropospheric O_3 associated with the small changes in NO_x (middle panel of Fig. 9a). Table 5 shows that integrating globally this equates to a Tg of O_3 (< 0.5 %) in the global tropospheric burden due to an increase in the turnover of Reactions (R1) and (R2) from the additional NO_x and HO_2 (from enhanced CO oxidation). For EMISDD Reaction (R10) suppresses O_3 formation by increasing the fraction of nitrogen lost to the surface and by decreasing the chain length of the NO_x recycling mechanism. Figure 9c shows the associated perturbations in OH in both simulations. A large fraction of chemical oxidation occurs in the tropical BL (Fiore et al., 2006) thus the increases in resident OH have a more marked effect on global atmospheric lifetimes than similar perturbations at higher latitudes. At other

latitudes changes in resident OH are in line with the changes in O_3 shown in Fig. 9b. The effect on tropospheric lifetimes is rather small as shown by the variability shown for both CO and CH_4 in Table 5. In summary the introduction of Reaction (R10) with a branching ratio of 0.3 % completely negates the increase in global oxidative capacity from ocean emissions of alkyl nitrates.

7 Conclusions

In this study we have examined the impact of introducing direct chemical formation of methyl nitrate (CH_3ONO_2) during NO_x recycling involving the methyl-peroxy radical on the global distribution of CH_3ONO_2, NO_x and tropospheric ozone. We compare this against the changes introduced from direct oceanic emission of CH_3ONO_2 and the higher alkyl nitrates in the tropics (10° S–10° N) based on a set of independent observations. It is found that the global surface distribution of CH_3ONO_2 is sensitive to the variability in the dry deposition velocity. Analysing the chemical budget reveals than ~ 50 % of nitrogen introduced via direct oceanic emission is lost by deposition processes close to the source regions which scales with the emission term, even when adopting conservative estimates for the dry deposition term. Given the lack of adequate chemical precursors in pristine locations, introducing a direct oceanic emission term for higher (C_2 and above) alkyl nitrates improves their distribution in the TM5 3-D global model when compared to independent aircraft measurements.

Using measurements taken at a variety of surface sites we show that applying the measured branching ratio of 1.0 % results in tropospheric mixing ratio of CH_3ONO_2 which are an order of magnitude too high. A previous estimate of the branching ratio (4.5×10^{-3}) derived from analysing chemical observations in the upper troposphere is also too low to be able to capture observed mixing ratios at the surface. However, adopting the lower limit for the branching ratio of 0.3 % allows the model to capture observed mixing ratios in the Southern Hemisphere without the need of any direct regional oceanic source term, as well as contributing to the observed mixing ratios in the

tropics resulting in a lower emission flux compared to that derived from observations alone. For the tropical upper troposphere a significant low model bias exists across a host of different sensitivity studies suggesting an as yet unknown missing chemical precursor source. For the upper troposphere in the northern sub-tropics, the seasonal and latitudinal distribution of NO_y is generally improved when including a mixture of direct emissions and chemical production, although similar improvements are also simulated when using a high oceanic emission term showing the need for tighter constraints on the strength of the emission source. In general alkyl nitrates account for between 5–10 % of the observed NO_y in the upper troposphere, being less important than either PAN or HNO_3.

Finally, in terms of tropospheric O_3, the increases which result from the additional nitrogen introduced by the direct emission of alkyl nitrates are essentially reversed at global scale when accounting for the sequestration of nitrogen due to the chemical formation of CH_3ONO_2.

From this study we recommend that in order to improve the understanding and modelling of alkyl nitrates in the future three main uncertainties are addressed. Firstly, further laboratory experiments should be performed to verify the chemical production of CH_3ONO_2 and provide an independent branching ratio, which can then lead to more concrete recommendations for atmospheric modellers. Secondly chemical measurements in the remote Southern Hemisphere above open water should be made to establish whether the direct oceanic flux only exists in the tropics. Thirdly the deposition of a range of alkyl nitrates should be determined to better constraint the efficiency of physical loss processes.

In terms of global modelling we suggest to include an oceanic flux for higher alkyl nitrates where we have shown that this improves the distribution of these important nitrogen reservoirs in the remote tropics. Ideally a future study could derive a parameterization for oceanic emissions related to the distribution of phykto-plancton blooms as measured from space and local wind speeds.

References

Atkinson, R.: Atmospheric chemistry of VOCs and NO_x, Atmos. Environ., 34, 2063–2101, 2000.

5   Atlas, E., Pollock, W., Greenberg, J., Heidt, L., and Thompson, A. M.: Alkyl nitrates, non-methane hydrocarbons and halocarbon gases over the equatorial Pacific Ocean during Saga 3, J. Geophys. Res., 98, 16933–16947, 1993.

Beyersdorf, A. J., Blake, D. R., Swanson, A., Meinardi, S., Rowland, F. S., and Davis, D.: Abundances and variability of tropospheric volatile organic compounds at the South Pole and

10   other Antarctic locations, Atmos. Environ., 44, 4565–4574, 2010.

Blake, N. J., Blake, D. R., Wingenter, O. W., Sive, B. C., Kang, C. H., Thornton, D. C., Bandy, A. R., Atlas, E., Flocke, F., Harris, J. M., and Rowland, F. S.: Aircraft measurements of the latitudinal, vertical and seasonal variations of NMHCs, methyl nitrate, methyl halides, and DMS during the First Aerosol Characterization Experiment (ACE 1), J. Geophys. Res.,

15   104, 21803–21817, 1999.

Blake, N. J., Blake, D. R., Swanson, A. L., Atlas, E., Flocke, F., and Rowland, F. S.: Latitudinal, vertical, and seasonal variations of C_1–C_4 alkyl nitrates in the troposphere over the Pacific Ocean during PEM-Tropics A and B: Oceanic and continental sources, J. Geophys. Res., 108, 8242, doi:10.1029/2001JD001444, 2003a.

20   Blake, N. J., Blake, D. R., Sive, B. C., Katzenstein, A. S., Meinardi, S., Wingenter, O. W., Atlas, E. L., Flocke, F., Ridley, B. A., and Rowland, F. S.: The seasonal evolution of NMHCs and light alkyl nitrates at middle to high northern latitudes during TOPSE, J. Geophys. Res., 108, 8359, doi:10.1029/2001JD001467, 2003b.

Boxe, C. S., Hamer, P. D., Ford, W., Hoffmann, M., and Shallcross, D. E.: The effect of the

25   novel $HO_2 + NO \rightarrow HNO_3$ reaction channel at South Pole, Antarctica, Antarct. Sci., 24, 417, doi:10.1017/S0954102012000144, 2012.

Brenninkmeijer, C. A. M., Crutzen, P., Boumard, F., Dauer, T., Dix, B., Ebinghaus, R., Filippi, D., Fischer, H., Franke, H., Frieß, U., Heintzenberg, J., Helleis, F., Hermann, M., Kock, H. H., Koeppel, C., Lelieveld, J., Leuenberger, M., Martinsson, B. G., Miemczyk, S., Moret, H. P.,

30   Nguyen, H. N., Nyfeler, P., Oram, D., O'Sullivan, D., Penkett, S., Platt, U., Pupek, M., Ra-

monet, M., Randa, B., Reichelt, M., Rhee, T. S., Rohwer, J., Rosenfeld, K., Scharffe, D., Schlager, H., Schumann, U., Slemr, F., Sprung, D., Stock, P., Thaler, R., Valentino, F., van Velthoven, P., Waibel, A., Wandel, A., Waschitschek, K., Wiedensohler, A., Xueref-Remy, I., Zahn, A., Zech, U., and Ziereis, H.: Civil Aircraft for the regular investigation of the atmosphere based on an instrumented container: The new CARIBIC system, Atmos. Chem. Phys., 7, 4953–4976, doi:10.5194/acp-7-4953-2007, 2007.

Browne, E. C. and Cohen, R. C.: Effects of biogenic nitrate chemistry on the NO_x lifetime in remote continental regions, Atmos. Chem. Phys., 12, 11917–11932, doi:10.5194/acp-12-11917-2012, 2012.

Buhr, M. P., Parrish, D. P., Norton, R. B., Fehsenfeld, F. C., Sievers, R. E., and Roberts, J. M.: Contribution of Organic Nitrates to the Total Reactive Nitrogen budget at a Rural Eastern US Site, J. Geophys. Res., 95, 9809–9816, 1990.

Butkovskaya, N. I., Kukui, A., Pouvesle, N., and Le Bras, G.: Formation of nitric acid in the gas-phase HO_2 + NO reaction: effects of temperature and water vapour, J. Phys. Chem. A., 109, 6509–6520, doi:10.1021/jp051534v, 2005.

Butkovskaya, N. I., Kukui, A., and Le Bras, G.: HNO_3 forming channel of the HO_2 + NO reaction as a function of pressure and temperature in the ranges of 72–600 Torr and 223–323 K, J. Phys. Chem. A., 111, 9047–9053, 2007.

Butkovskaya, N. I., Rayez, M.-T., Kukui, A., and Le Bras, G.: Water Vapor Effect on the HNO_3 Yield in the HO_2 + NO reaction: experimental and theoretical evidence, J. Phys. Chem. A., 113, 11327–11342, doi:10.1021/jp811428p, 2009.

Butkovskaya, N. I., Kukui, A., and Le Bras, G.: Pressure and temperature dependence of ethyl nitrate formation in the $C_2H_5O_2$ + NO reaction, J. Phys. Chem. A, 114, 956–964, doi:10.1021/jp910003a, 2010.

Butkovskaya, N. I., Kukui, A., and Le Bras, G.: Pressure and temperature dependence of methyl nitrate formation in the CH_3O_2 + NO reaction, J. Phys. Chem. A, 116, 5972–5980, doi:10.1021/jp210710d, 2012.

Cariolle, D., Evans, M. J., Chipperfield, M. P., Butkovskaya, N., Kukui, A., and Le Bras, G.: Impact of the new HNO_3-forming channel of the HO_2 + NO reaction on tropospheric HNO_3, NO_x, HO_x and ozone, Atmos. Chem. Phys., 8, 4061–4068, doi:10.5194/acp-8-4061-2008, 2008.

Chuck, A. L., Turner, S. M., and Liss, P. S.: Direct evidence for a marine source of C_1 and C_2 alkyl nitrates, Science, 297, 1151–1154, 2002.

The impact of the chemical production of methyl nitrate

J. E. Williams et al.

Title Page

| Abstract | Introduction |

| Conclusions | References |

| Tables | Figures |

◄ | ►

◄ | ►

Back | Close

Full Screen / Esc

Printer-friendly Version

Interactive Discussion

Clemitshaw, K. C., Williams, J., Rattigan, O. V., Shallcross, D. E., Law, K. S., and Cox, R. A.: Gas-phase ultraviolet absorption cross-sections and atmospheric lifetimes of several C_2–C_5 alkyl nitrates, J. Photochem. Photobiol. A, 102, 117–126, 1997.

Dahl, E. E. and Saltzman, E. S.: Alkyl nitrate photochemical production rates in North Pacific seawater, Mar. Chem., 112, 137, doi:10.1016/j.marchem.2008.10.002, 2008.

Dahl, E. E., Saltzman, E. S., and de Bruyn, W. J.: The aqueous phase yield of alkyl nitrates from ROO + NO: implications for photochemcial production in seawater, Geophys. Res. Letts., 30, 1271, doi:10.1029/2002GL016811, 2003.

Dahl, E. E., Yvon-Lewis, S. A., and Saltzman, E. S.: Saturation anomalies of alkyl nitrates in the tropical Pacific Ocean, Geophys. Res. Lett., 32, L20817, doi:10.1029/2005GL023896, 2005.

Dahl, E. E., Yvon-Lewis, S. A., and Saltzman, E. S.: Alkyl nitrate (C_1–C_3) depth profiles in the tropical Pacific Ocean, J. Geophys. Res., 112, C01012, doi:10.1029/2006JC003471, 2007.

Dee, D. P., Uppala, S. M., Simmons, A. J., Berrisford, P., Poli, P., Kobayashi, S., Andrae, U., Balmaseda, M. A., Balsamo, G., Bauer, P., Bechtold, P., Beljaars, A. C. M., van de Berg, L., Bidlot, J., Bormann, N., Delsol, C., Dragani, R., Fuentes, M., Geer, A. J., Haimberger, L., Healy, S. B., Hersbach, H., Hólm, E. V., Isaksen, L., Kållberg, P., Köhler, M., Matricardi, M., McNally, A. P., Monge-Sanz, B. M., Morcrette, J.-J., Park, B.-K., Peubey, C., de Rosnay, P., Tavolato, C., Thépaut, J.-N., and Vitart, F.: The ERA-Interim reanalysis: configuration and performance of the data assimilation system, Q. J. Roy. Meteorol. Soc., 137, 553–597, 2011.

Farmer, D. K., Perring, A. E., Wooldridge, P. J., Blake, D. R., Baker, A., Meinardi, S., Huey, L. G., Tanner, D., Vargas, O., and Cohen, R. C.: Impact of organic nitrates on urban ozone production, Atmos. Chem. Phys., 11, 4085–4094, doi:10.5194/acp-11-4085-2011, 2011.

Fehsenfeld, F. C., Daum, P., Leaitch, W. R., Trainer, M., Parrish, D. D., and Hübler, G.: Transport and processing of O_3 and O_3 precursors over the North Atlantic: an overview of the 1993 North Atlantic Regional Experiment (NARE) summer intensive, J. Geophys. Res., 101, 28877–28891, 1996.

Fiore, A. M., Horowitz, L. W., Dlugokencky, E. J., and West, J. J.: Impact of meteorology and emissions on methane trends, 1990–2004, Geophys. Res. Lett., 33, L12809, doi:10.1029/2006GL026199, 2006.

Flocke, F., Atlas, E., Madronich, S., Schauffler, S. M., Aikin, K., Margitan, J. J., and Bui, T. P.: Observations of methyl nitrate in the lower stratosphere during STRAT: Implications for gas phase prodcution mechanisms, Geophys. Res. Lett., 25, 1891–1894, 1998a.

The impact of the chemical production of methyl nitrate

J. E. Williams et al.

Title Page

Abstract | Introduction

Conclusions | References

Tables | Figures

|◄ | ►|

◄ | ►

Back | Close

Full Screen / Esc

Printer-friendly Version

Interactive Discussion

Flocke, F., Volz-Thomas, A., Buers, H.-J., Pätz, W., Garthe, H.-J., and Kley, D.: Long-term measurements of alkyl nitrates in southern Germany: 1. General behavior and seasonal and diurnal variation, J. Geophys. Res., 103, 5279–5746, 1998b.

Fortuin, J. P. F. and Kelder, H.: An ozone climatology based on ozonesonde and satellite measurements, J. Geophys. Res., 103, 31709–31734, 1998.

Ganzeveld, L. and Lelieveld, J.: Dry deposition parameterization in a chemistry general circulation model and its influence on the distribution of reactive gases, J. Geophys. Res., 100, 20999–21012, 1995.

Gery, M. W., Whitten, G. Z., Killus, J. P., and Dodge, M. C.: A photochemical kinetics mechanism for urban and regional scale computer modeling, J. Geophys. Res., 94, 925–956, 1989.

Granier, C., Bessagnet, B., Bond, T., D'Aniola, A., Denier von der Gon, H., Frost, G. J., Heil, A., Kaiser, J. W., Kinne, S., Klimont, Z., Kloster, S., Lamarque, J.-F., Liousse, C., Masui, T., Meleuax, F., Mieville, A., Ohara, T., Raut, J.-C., Riahi, K., Schultz, M. G., Smith, S. J., Thompson, A., van Aardenne, J., van der Werf, G. R., and van Vuuren, D. P.: Evolution of anthropogenic and biomass burning emission of air pollutants at global and regional scales during the 1980–2010 period, Climatic Change, 109, 163–190, doi:10.1007/s10584-011-0154-1, 2011.

Gottschaldt, K., Voigt, C., Jöckel, P., Righi, M., Deckert, R., and Dietmüller, S.: Global sensitivity of aviation NO_x effects to the HNO_3-forming channel of the HO_2 + NO reaction, Atmos. Chem. Phys., 13, 3003–3025, doi:10.5194/acp-13-3003-2013, 2013.

Guenther, A., Karl, T., Harley, P., Wiedinmyer, C., Palmer, P. I., and Geron, C.: Estimates of global terrestrial isoprene emissions using MEGAN (Model of Emissions of Gases and Aerosols from Nature), Atmos. Chem. Phys., 6, 3181–3210, doi:10.5194/acp-6-3181-2006, 2006.

Gupta, M. L., Cicerone, R. J., Blake, D. R., Rowland, F. S., and Isaksen, I. S. A.: Global atmospheric distributions and source strengths of light hydrocarbons and tetrachloroethene, J. Geophys. Res., 103, 28219–28325, 1998.

Hauglustaine, D., Lathiére, A., Szopa, S., and Folberth, G. A.: Future tropospheric ozone simulated with a climate-chemistry-biosphere model, Geophys. Res. Lett., 32, L24807, doi:10.1029/2005GL024031, 2005.

Hertel, O., Berkowicz, R., and Christensen, J.: Test of two numerical schemes for use in atmospheric transport-chemistry models, Atmos. Environ., 27, 2591–2611, 1993.

The impact of the chemical production of methyl nitrate

J. E. Williams et al.

Title Page

Abstract | Introduction

Conclusions | References

Tables | Figures

|◀ | ▶|

◀ | ▶

Back | Close

Full Screen / Esc

Printer-friendly Version

Interactive Discussion

Huijnen, V., Williams, J., van Weele, M., van Noije, T., Krol, M., Dentener, F., Segers, A., Houwel-ing, S., Peters, W., de Laat, J., Boersma, F., Bergamaschi, P., van Velthoven, P., Le Sager, P., Eskes, H., Alkemade, F., Scheele, R., Nédélec, P., and Pätz, H.-W.: The global chemistry transport model TM5: description and evaluation of the tropospheric chemistry version 3.0, Geosci. Model Dev., 3, 445–473, doi:10.5194/gmd-3-445-2010, 2010.

Jaffe, D., Mahura, A., Kelly, J., Atkins, J., Novelli, P. C., and Merrill, J.: Impact of Asian emissions on the remote North Pacific atmosphere: interpretation of CO data from Shemya, Guam, Mid-way and Mauna Loa, J. Gephys. Res., 102, 28627–28635, doi:10.1029/96JD02750, 1997.

Jégou, F., Urban, J., de La Noë, J., Ricaud, P., Le Flochmoën, E., Murtagh, D. P., Eriks-son, P., Jones, A., Petelina, S., Llewellyn, E. J., Lloyd, N. D., Haley, C., Lumpe, J., Ran-dall, C., Bevilacqua, R. M., Catoire, V., Huret, N., Berthet, G., Renard, J. B., Strong, K., Davies, J., Mc Elroy, C. T., Goutail, F., and Pommereau, J. P.: Technical Note: Validation of Odin/SMR limb observations of ozone, comparisons with OSIRIS, POAM III, ground-based and balloon-borne instruments, Atmos. Chem. Phys., 8, 3385–3409, doi:10.5194/acp-8-3385-2008, 2008.

Jones, A. E., Wolff, E. W., Ames, D., Bauguitte, S. J.-B., Clemitshaw, K. C., Fleming, Z., Mills, G. P., Saiz-Lopez, A., Salmon, R. A., Sturges, W. T., and Worton, D. R.: The multi-seasonal NO_y budget in coastal Antarctica and its link with surface snow and ice core nitrate: results from the CHABLIS campaign, Atmos. Chem. Phys., 11, 9271–9285, doi:10.5194/acp-11-9271-2011, 2011.

Kames, J. and Schurath, U.: Alkyl nitrates and bifunctional nitrates of atmospheric interest: Henry's law constants and their temperature dependencies, J. Atmos. Chem., 15, 79–95, 1992.

Lamarque, J.-F., Bond, T. C., Eyring, V., Granier, C., Heil, A., Klimont, Z., Lee, D., Liousse, C., Mieville, A., Owen, B., Schultz, M. G., Shindell, D., Smith, S. J., Stehfest, E., Van Aar-denne, J., Cooper, O. R., Kainuma, M., Mahowald, N., McConnell, J. R., Naik, V., Riahi, K., and van Vuuren, D. P.: Historical (1850–2000) gridded anthropogenic and biomass burn-ing emissions of reactive gases and aerosols: methodology and application, Atmos. Chem. Phys., 10, 7017–7039, doi:10.5194/acp-10-7017-2010, 2010.

Lambert, G. and Schmidt, S.: Re-evaluation of the oceanic flux of methane uncertainties and long-term variations, Chemosphere, 26, 579–589, 1993.

Luo, G. and Yu, F.: A numerical evaluation of global oceanic emissions of α-pinene and iso-prene, Atmos. Chem. Phys., 10, 2007–2015, doi:10.5194/acp-10-2007-2010, 2010.

The impact of the chemical production of methyl nitrate

J. E. Williams et al.

Title Page

Abstract	Introduction
Conclusions	References
Tables	Figures

Back | Close

Full Screen / Esc

Printer-friendly Version

Interactive Discussion

Meijer, E. W., van Velthoven, P. F. J., Brunner, D. W., Huntrieser, H., and Kelder, H.: Improvement and evaluation of the parameterisation of nitrogen oxide production by lightning, Phys. Chem. Earth, 26, 557–583, 2001.

Neu, J. L., Lawler, M. J., Prather, M. J., and Saltzman, E. S.: Oceanic alkyl nitrates as a natural source of tropospheric ozone, Geophys. Res. Lett., 35, L13814, doi:10.1029/2008GL034189, 2008.

Ohara, T., Akimoto, H., Kurokawa, J., Horii, N., Yamaji, K., Yan, X., and Hayasaka, T.: An Asian emission inventory of anthropogenic emission sources for the period 1980–2020, Atmos. Chem. Phys., 7, 4419–4444, doi:10.5194/acp-7-4419-2007, 2007.

Orlando, J. J., Tyndall, G. S., and Calvert, J. G.: Thermal decomposition pathways for peroxy-acetyl nitrate (PAN): implications for atmospheric methyl nitrate levels, Atmos. Environ., 26, 3111–3118, 1992.

Marenco, A., Thouret, V., Nédélec, P., Smit, H., Helten, M., Kley, D., Karcher, F., Simon, P., Law, K., Pyle, J., Poschmann, G., von Wrede, R., Hume, C., and Cook, T.: Measurement of ozone and water vapor by Airbus in-service aircraft: the MOZAIC airborne program, an overview, J. Geophys. Res., 103, 25631–25642, 1998.

Ordóñez, C., Elguindi, N., Stein, O., Huijnen, V., Flemming, J., Inness, A., Flentje, H., Ka-tragkou, E., Moinat, P., Peuch, V.-H., Segers, A., Thouret, V., Athier, G., van Weele, M., Zerefos, C. S., Cammas, J.-P., and Schultz, M. G.: Global model simulations of air pollution during the 2003 European heat wave, Atmos. Chem. Phys., 10, 789–815, doi:10.5194/acp-10-789-2010, 2010.

Pfister, G. G., Emmons, L., Hess, P. G., Lamarque, J.-F., Orlando, J. J., Walters, S., Guen-ther, A., Palmer, P. I., and Lawrence, P. J.: Contribution of isoprene to chemical budgets: a model tracer study with the NCAR CTM MOZART-4, J. Geophys. Res., 113, D05308, doi:10.1029/2007JD008948, 2008.

Raper, J. L., Kleb, M. M., Jacob, D. J., Davis, D. D., Newell, R. E., Fuelberg, H. E., Ben-dura, R. J., Hoell, J. M., and McNeal, R. J.: Pacific Exploratory Mission in the Trop-ical Pacific: PEM-Tropics B, March–April 1999, J. Geophys. Res., 106, 32401–32425, doi:10.1029/2000JD900833, 2001.

Ridley, B. A. and Robinson, E.: The Mauna Loa Observatory Photochemical Experiment, J. Geophys. Res., 97, 10285–10290, 1992.

Reeves, C. E., Slemr, J., Oram, D. E., Worton, D., Penkett, S. A., Stewart, D. J., Purvis, R., Watson, N., Hopkins, J., Lewis, A., Methven, J., Blake, D. R., and Atlas, E.: Alykl nitrates

The impact of the chemical production of methyl nitrate

J. E. Williams et al.

Title Page

Abstract	Introduction
Conclusions	References
Tables	Figures

|◄ | ►|

◄ | ►

Back | Close

Full Screen / Esc

Printer-friendly Version

Interactive Discussion

in outflow from North America over the North Atlantic during Intercontinental Transport of Ozone and Precursors 2004, J. Geophys. Res., 112, doi:10.1029/2006JD007567, 2007.

Roberts, J. M., Bertman, S. B., Parrish, D. D., Fehsenfeld, F. C., Jobson, B. T., and Niki, H.: Measurement of alkyl nitrates at Chebogue Point, Nova Scotia during the 1993 North Atlantic Regional Experiment (NARE) intensive, J. Geophys. Res., 103, 13569–13580, 1998.

Rudolph, J. and Ehhalt, D. H.: Measurements of C_2–C_5 hydrocarbons over the North Atlantic, J. Geophys. Res., 86, 11959–11964, 1981.

Russo, R. S., Zhou, Y., Haase, K. B., Wingenter, O. W., Frinak, E. K., Mao, H., Talbot, R. W., and Sive, B. C.: Temporal variability, sources, and sinks of C_1–C_5 alkyl nitrates in coastal New England, Atmos. Chem. Phys., 10, 1865–1883, doi:10.5194/acp-10-1865-2010, 2010.

Sander, S. P., Abbatt, J. R., Burkholder, J. B., Friedl, R. R., Golden, D. M., Huie, R. E., Kolb, C. E., Kurylo, G., Moortgat, K., Orkin, V. L., and Wine, P. H.: Chemical Kinetics and Photochemical Data for Use in Atmospheric Studies, Evaluation No.17, JPL Publication 10–6, Jet Propulsion Laboratory, Pasadena, available at: http://jpldataeval.jpl.nasa.gov (last access: July 2013), 2011.

Sanderson, M. G., Collins, W. J., Derwent, R. G., and Johnson, C. E.: Simulation of global hydrogen levels using a Lagrangian three-dimensional model, J. Atmos. Chem., 46, 15–48, 2003.

Schuck, T. J., Brenninkmeijer, C. A. M., Baker, A. K., Slemr, F., von Velthoven, P. F. J., and Zahn, A.: Greenhouse gas relationships in the Indian summer monsoon plume measured by the CARIBIC passenger aircraft, Atmos. Chem. Phys., 10, 3965–3984, doi:10.5194/acp-10-3965-2010, 2010.

Schultz, M. G., Backman, L., Balkanski, Y., Bjoerndalsaeter, S., Brand, R., Burrows, J. P., Dalsøeren, S., de Vasconcelos, M., Grodtmann, B., Hauglustaine, D. A., Heil, A., Hoelzemann, J. J., Isaksen, I. S. A., Kaurola, J., Knorr, W., Ladstaetter-Weissenmayer, A., Mota, B., Oom, D., Pacyna, J., Panasiuk, D., Pereira, J. M. C., Pulles, T., Pyle, J., Rast, S., Richter, A., Savage, N., Schnadt, C., Schultz, M., Spessa, A., Staehelin, J., Sundet, J. K., Szopa, S., Thonicke, K., van het Bolscher, M., van Noije, T., van Velthoven, P., Vik, A. F., and Wittrock, F.: REanalysis of the TROpospheric chemical composition over the past 40 yr (RETRO) – a long-term global modeling study of tropospheric chemistry, Final Report, Jülich/Hamburg, Germany, 2007 (Published as report no. 48/2007 in the series "Reports on Earth System Science" of the Max Planck Institute for Meteorology, Hamburg, ISSN 1614–1199, 2007).

Title Page

Abstract | Introduction

Conclusions | References

Tables | Figures

|◀ | ▶|

◀ | ▶

Back | Close

Full Screen / Esc

Printer-friendly Version

Interactive Discussion

Simpson, I. J., Meinardi, S., Blake, D. R., Blake, N. J., Rowland, F. S., Atlas, E., and Flocke, F.: A biomass burning source of C_1–C_4 alkyl nitrates, Geophys. Res. Lett., 29, 2168, doi:10.1029/2002GL016290, 2002.

Søvde, O. A., Hoyle, C. R., Myrhe, G., and Isaksen, I. S. A.: The HNO_3 forming branch of the HO_2 + NO reaction: pre-industrial-to-present trands in atmospheric species and radiative forcings, Atmos. Chem. Phys., 11, 8929–8943, doi:10.5194/acp-11-8929-2011, 2011.

Spahni, R., Wania, R., Neef, L., van Weele, M., Pison, I., Bousquet, P., Frankenberg, C., Foster, P. N., Joos, F., Prentice, I. C., and van Velthoven, P.: Constraining global methane emissions and uptake by ecosystems, Biogeosciences, 8, 1643–1665, doi:10.5194/bg-8-1643-2011, 2011.

Stevenson, D. S., Dentener, F. J., Schultz, M. G., Ellington, K., van Noije, T. P. C., Wild, O., Zeng, G., Amann, M., Atherton, C. S., Bell, N., Bergmann, D. J., Bey, I., Butler, T., Cofala, J., Collins, W. J., Derwent, R. G., Doherty, R. M., Brevet, J., Eskes, H. J., Fiore, A. M., Gauss, M., Hauglustaine, D. A., Horowitz, L. W., Isaksen, I. S. A., Krol, M. C., Lamarque, J.-F., Lawrence, M. G., Montanaro, V., Müller, J.-F., Pitari, G., Prather, M. J., Pyle, J. A., Rast, S., Rodriguez, J. M., Sanderson, M. G., Savage, N. H., Shindell, D. T., Strahan, S. E., Sudo, K., and Szopa, S.: Multimodel ensemble simulations of present-day and near-future tropospheric ozone, J. Geophys. Res., 111, D08301, doi:10.1029/2005JD006338,2006.

Swanson, A. L., Blake, N. J., Atlas, E., Flocke, F., Blake, D. R., and Rowland, F. S.: Seasonal variations of C_2–C_4 nonmethane hydrocarbons and C_1–C_4 alkyl nitrates at the Summit research station in Greenland, J. Geophys. Res., 108, 4065, doi:10.1029/2001JD001445, 2003.

Swanson, A. L., Davis, D. D., Arimoto, R., Roberts, P., Atlas, E. L., Flocke, F., Meinardi, S., Rowland, F. S., and Blake, D. R.: Organic trace gases of oceanic origin observed at South Pole during ISCAT 2000, Atmos. Environ., 38, 5463–5472, 2004.

Talukdar, R. K., Herndon, S. C., Burkholder, J. B., Roberts, J. M., and Ravishankara, A. R.: Atmospheric fate of several alkyl nitrates, Part 1: Rate coefficients of the reactions of alkyl nitrates with isotopically labelled hydroxyl radicals, J. Chem. Soc. Faraday Trans., 93, 2787–2796, 1997a.

Talukdar, R. K., Burkholder, J. B., Hunter, M., Gilles, M. K., Roberts, J. M., and Ravishankara, A. R.: Atmospheric fate of several alkyl nitrates, Part 2: UV absorption cross-sections and photodissociation quantum yields, J. Chem. Soc. Faraday Trans., 93, 2797–2805, 1997b.

The impact of the chemical production of methyl nitrate

J. E. Williams et al.

Title Page

Abstract	Introduction
Conclusions	References
Tables	Figures

◄◄   ►►

◄   ►

Back   Close

Full Screen / Esc

Printer-friendly Version

Interactive Discussion

Thouret, V., Marenco, A., Logan, J. A., Nédélec, P., and Grouhel, C.: Comparisons of ozone measurements from the MOZAIC airborne program and the ozone sounding network at eight locations, J. Geophys. Res., 103, 25695–25720, 1998.

Urban, J., Pommier, M., Murtagh, D. P., Santee, M. L., and Orsolini, Y. J.: Nitric acid in the stratosphere based on Odin observations from 2001 to 2009 – Part 1: a global climatology, Atmos. Chem. Phys., 9, 7031–7044, 2009,
http://www.atmos-chem-phys.net/9/7031/2009/.

van der A, R. J., Allaart, M. A. F., and Eskes, H. J.: Multi sensor reanalysis of total ozone, Atmos. Chem. Phys., 10, 11277–11294, doi:10.5194/acp-10-11277-2010, 2010.

Walega, J. G., Ridley, B. A., Madronich, S., Grahek, F. E., Shetter, D., Sauvain, T. D., Hahn, C. J., Merill, J. T., Bodhaine, B. A., and Robinson, E.: Observations of peroxyacetyl nitrate, peroxypropionyl nitrate, methyl nitrate and ozone during the Mauna Loa Observatory Photochemical Experiment, J. Geophys, Res., 97, 10311–10330, 1992.

Wang, Y., Choi, Y., Zeng, T., Davis, D., Buhr, M., Huey, L. G., and Neff, W.: Assessing the photochemical impact of snow NO_x emissions over Anarctica during ANTCI 2003, Atmos. Environ., 41, 3944–3958, 1007.

Weller, R., Jones, A. E., Wille, A., Jacobi, H.-W., McIntyre, H. P., Sturges, W. T., Huke, M., and Wahenbach, D.: Seasonality of reactive nitrogen oxides (NO_y) at Neumayer Station, Antarctica, J. Geophys. Res., 107, D234673, doi:10.1029/2002JD002495, 2002.

Williams, J. E. and van Velthoven, P. F. J.: Uncertainty in the future distribution of tropospheric ozone over West Africa due to variability in anthropogenic emissions estimates between 2025 and 2050, Int. J. Geophys., 10, 324359, doi:10.1155/2011/324359, 2011.

Williams, J. E., van Velthoven, P. F. J., and Brenninkmeijer, C. A. M.: Quantifying the uncertainty in simulating global tropospheric composition due to the variability in global emission estimates of Biogenic Volatile Organic Compounds, Atmos. Chem. Phys., 13, 2857–2891, doi:10.5194/acp-13-2857-2013, 2013.

Yonemura, S., Kawashima, S., and Tsuruta, H.: Carbon monoxide, hydrogen and methane uptake by soils in a temperate arable field and a forest, J. Geophys. Res.-Atmos., 105, 14347–14362, 2000.

Title Page

Abstract | Introduction

Conclusions | References

Tables | Figures

◀ | ▶

◀ | ▶

Back | Close

Full Screen / Esc

Printer-friendly Version

Interactive Discussion

Table 1a. Mixing ratios of CH_3ONO_2 measured at the surface over the last few decades.

Region	Latitude	Lat/Lon	Mixing ratios (ppt)	Reference
NH	73° N	38° W	~ 4	Swanson et al. (2003)
	44° N	66° W	~ 2	Roberts et al. (1998)
Tropics	20° N	156° W	~ 4	Walega et al. (1992)
	0–17° N	150° E–150° W	2–50	Dahl et al. (2005)
	18° S–30° N	50° W–5° E	4–40	Chuck et al. (2002)
	16–24° S	133–145° E	~ 5	Simpson et al. (2002)
SH	70° S	8° W	8–10	Weller et al. (2002)
	75.4° S	26.4° W	2–14	Jones et al. (2011)
	88–90° S	ALL	~ 3–11	Swanson et al. (2004)
	88–90° S	ALL	~ 4–13	Beyersdorf et al. (2010)

Table 1b. The range of CH_3ONO_2 mixing ratios measured in the FT (between 2 and 10 km) during research flights over the last few decades from various measurement campaigns.

Region	Latitude	Longitude	Mixing ratios (ppt)	Reference
NH	40–85° N	60–110° W	~ 2–4	Blake et al. (2003b)
	30–40° N	20–40° W	~ 2–3	Reeves et al. (2007)
Tropics/Mid Lat	2° S–60° N	115–155° W	~ 3–4	Flocke et al. (1998a)
	40° S–40° N	150° E-140° W	1–27	Blake et al. (2003a)
Global	60° S–80° N	160° E–150° W	~ 3–40	Blake et al. (1999)

Table 2. An overview of the sensitivity studies performed with TM5 to investigate the impact of the chemical production of CH_3ONO_2 on global tropospheric composition.

Model simulation	Direct oceanic emissions	Branching ratio	Comments
BASE	NO	N/A	Default modified CB05 chemistry without CH_3ONO_2 and no oceanic emissions
EMISS	YES	N/A	Adopting the emission estimates for CH_3ONO_2 from Neu et al. (2008) between 10° S–10° N
DEMISS	YES	N/A	Adopting an emission twice that of Neu et al. (2008) between 10° S–10° N
LOWBR	NO	0.3 %	Lower uncertainty range from Butkovskaya et al. (2012)
HIGHBR	NO	1.0 %	Branching ratio measured by Butkovskaya et al. (2012)
EMISSPT	YES	0.3 %	Combined emissions and direct production
EMISSDD	YES	0.3 %	As EMISSPT except the dry deposition flux is increased by 100 %
FLIGHT	YES	0.045 %	As LOWBR except adopting the branching ratio suggested in Flocke et al. (2008) derived from measurements

Table 3. The annual tropospheric chemical budget terms for CH_3ONO_2 for 2008 given in $Tg N yr^{-1}$ for selected simulations.

	EMISS	DEMISS	EMISSPT	EMISSDD	FLIGHT
Emission	0.286	0.573	0.143	0.143	0.143
$NO + CH_3O_2$	N/A	N/A	0.995	0.993	0.074
$OH + CH_3ONO_2$	0.011	0.022	0.053	0.042	0.009
$CH_3ONO_2 + h\nu$	0.122	0.243	0.532	0.429	0.097
Dry Deposition	0.143	0.285	0.511	0.632	0.106
Wet Deposition	0.008	0.017	0.035	0.027	0.007

Table 4. The annual tropospheric chemical budget terms for ORGNTR for 2008 as calculated in the modified CB05 chemical mechanism as given in $TgN\,yr^{-1}$ for selected TM5 simulations. The term for total nitrogen deposition is defined as the sum of dry and wet deposition of NO_2, HNO_3, ORGNTR and PAN.

	BASE	EMISSDD
Emission	N/A	0.168
$NO + XO_2N$	11.261	11.251
$NO_3 + C_3H_6$	0.054	0.054
$NO_3 + ISOP$	2.256	2.243
$NO_3 + TERP$	0.981	0.978
$OH + ORGNTR$	1.258	1.286
$ORGNTR + h\nu$	4.380	4.490
Dry deposition	3.021	3.100
Wet deposition	6.175	6.317
Global burden	0.168	0.172
Total N deposition	48.418	48.590

Table 5. The annual global chemical budget terms for tropospheric O_3 given in $Tg\,O_3\,yr^{-1}$ for selected simulations.

	BASE	EMISS	EMISSPT	EMISSDD
$NO + HO_2$	2929.9	2941.0	2924.7	2919.6
$NO + CH_3O_2$	1130.6	1137.0	1125.7	1122.9
$NO + XO_2$	458.7	459.0	458.1	458.0
Total	4518.7	4537.0	4508.5	4500.5
Dry Deposition	846.9	848.3	845.3	844.6
Trop. Burden	328.6	329.6	328.9	328.4
Trop. CO lifetime (days)	51.07	50.76	51.03	51.13
Trop. CH_4 lifetime (yr)	8.15	8.11	8.17	8.18
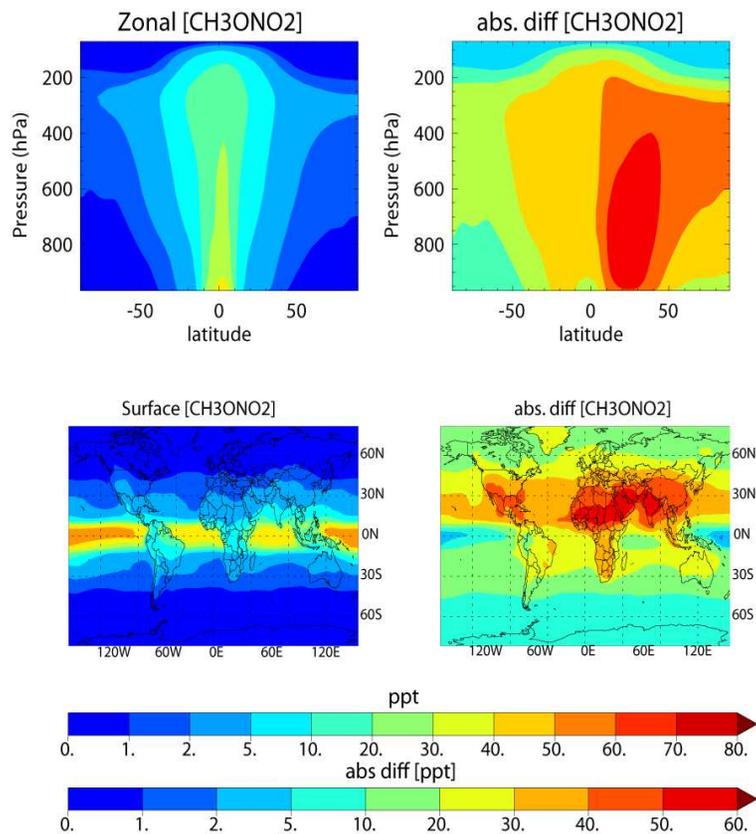
Fig. 1. The annual mean distribution in CH$_3$ONO$_2$ during 2008. Both the zonal and horizontal means are shown (top and bottom, respectively) for EMISS. The right panels show the absolute differences for EMISSPT-EMISS given in ppt.
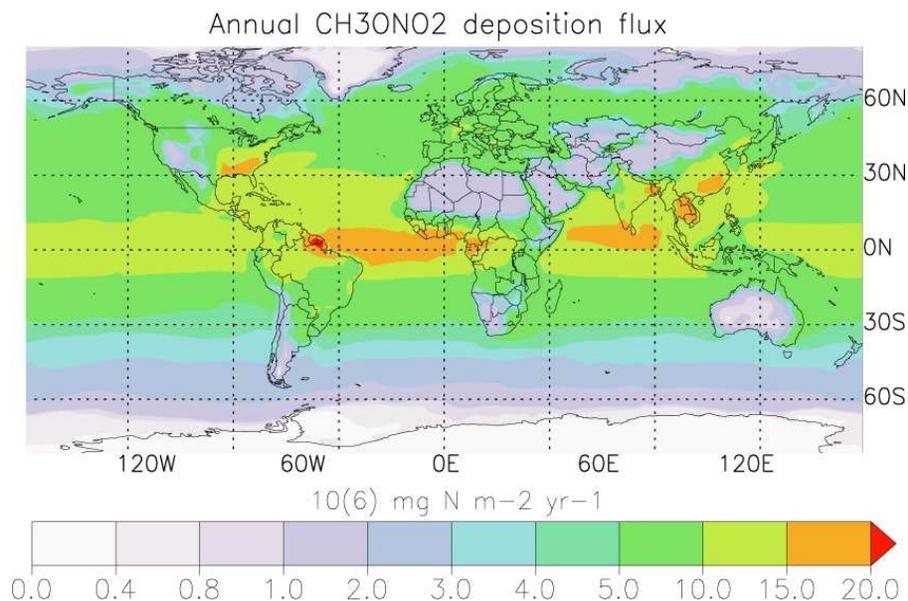
Fig. 2. The annually integrated global deposition flux of CH_3ONO_2 during 2008 from EMISSPT. The values are given in $106\,mg\,N\,m^{-2}\,yr^{-1}$.
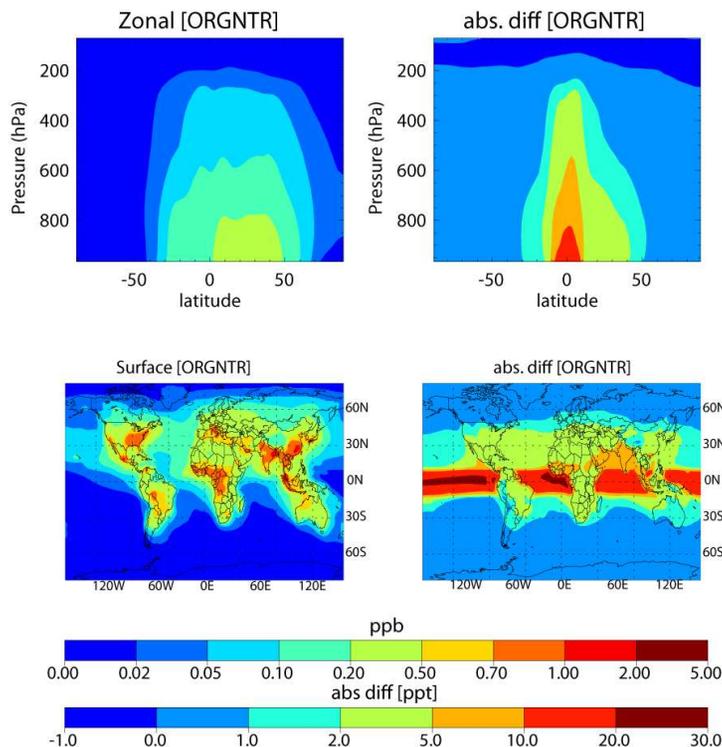
Fig. 3. The annual global distribution in ORGNTR during 2008 given in ppb. Both the zonal and horizontal (< 800 hPa) means are shown (top and bottom, respectively) for the BASE simulation. The absolute differences when compared against the EMISSPT simulation are also given, with differences being in the ppt range.
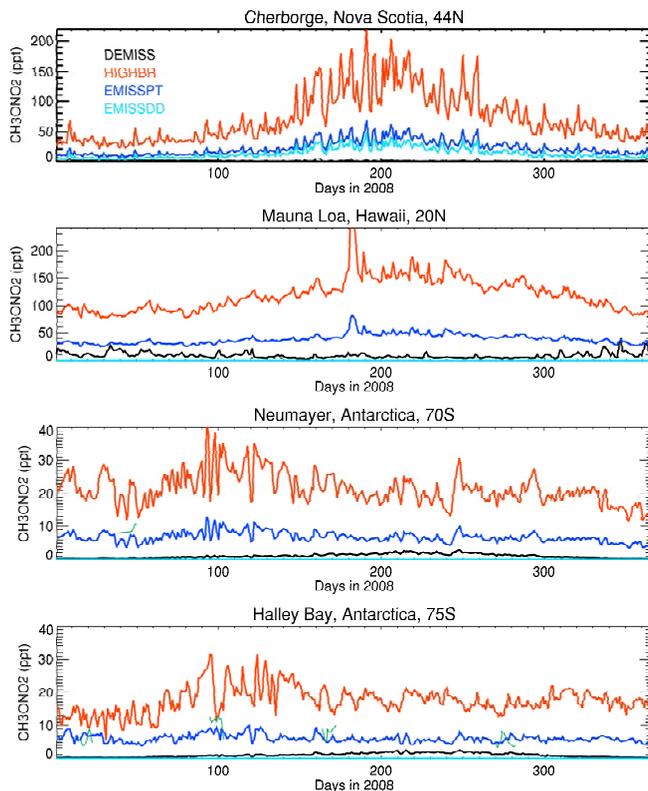
Fig. 4. Daily mean mixing ratios of CH_3ONO_2 in the DEMISS, HIGHBR, EMISSPT and EMISSDD simulations extracted at Cherborge ($45°$ N, top), Mauna Loa ($20°$ N, top middle), Neumayer ($70°$ S, bottom middle) and Halley Bay ($75°$ S, bottom). When the scale allows we also show the observed mixing ratios of CH_3ONO_2 available in the literature (green, see text for details). The simulations shown are EMISS (black), HIGHBR (red), EMISSPT (dark blue) and EMISSDD (cyan).

Title Page

Abstract | Introduction

Conclusions | References

Tables | Figures

|◀ | ▶|

◀ | ▶

Back | Close

Full Screen / Esc

Printer-friendly Version

Interactive Discussion
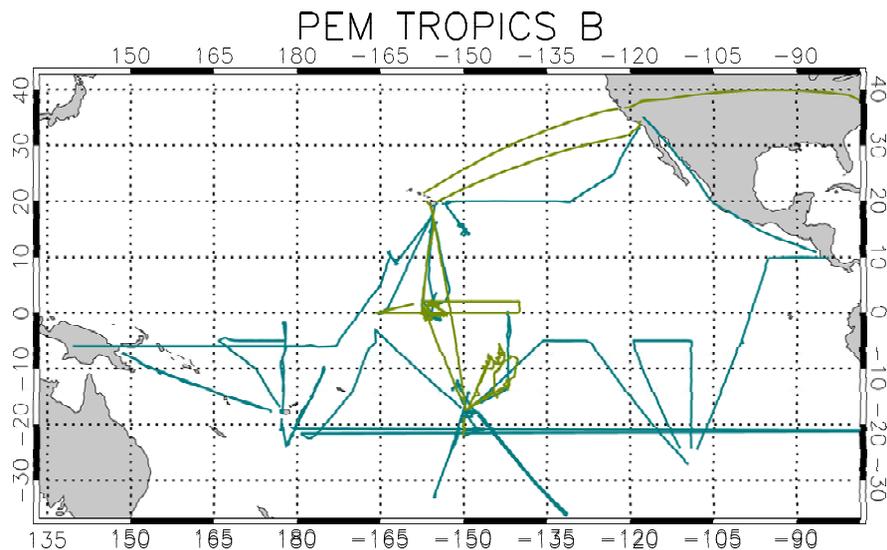
Fig. 5. The flight routes of taken by the DC-8 (cyan) and P-3B (Green) during March 1999 as part of the PEM-B Tropics campaign.

Discussion Paper | Discussion Paper | Discussion Paper | Discussion Paper

ACPD

13, 20111–20163, 2013

The impact of the chemical production of methyl nitrate

J. E. Williams et al.

Title Page

Abstract | Introduction

Conclusions | References

Tables | Figures

|◄ | ►|

◄ | ►

Back | Close

Full Screen / Esc

Printer-friendly Version

Interactive Discussion
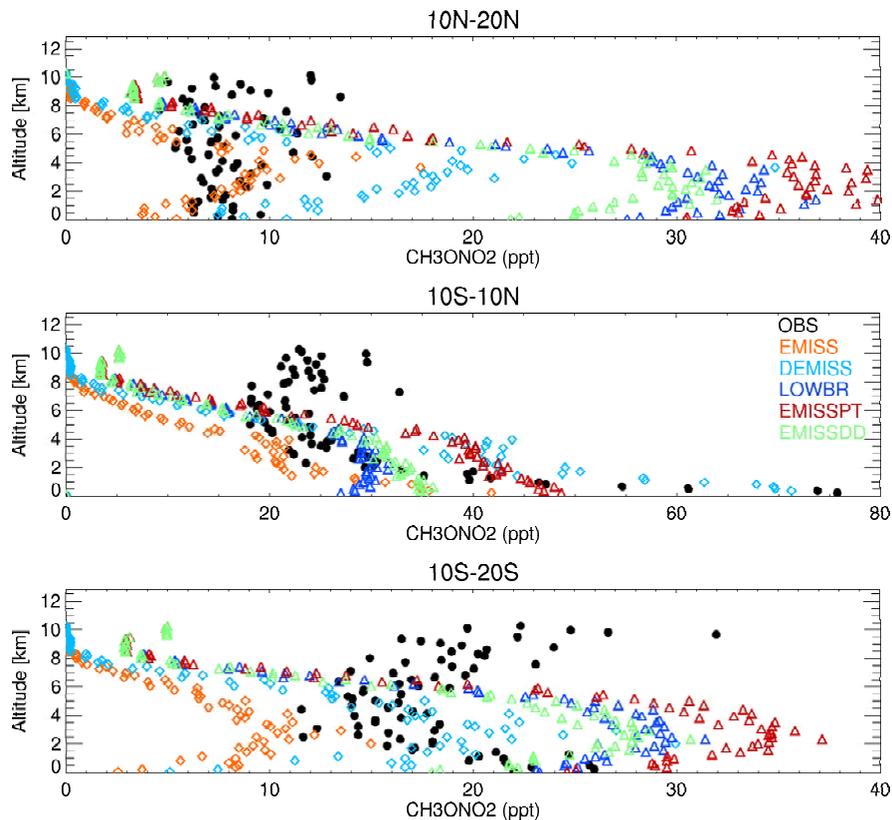
Fig. 6. A comparison of the distribution of CH_3ONO_2 around the tropical Pacific Ocean as measured during March 1999 in the PEM-Tropics B measurement campaign and simulated in TM5. Comparisons are shown for EMISS (orange), DEMISS (blue), P_T_pt03 (dark blue), EMISSPT (red) and EMISSDD (azure green). The reader should note the different scales on the x-axis between latitudinal regions.
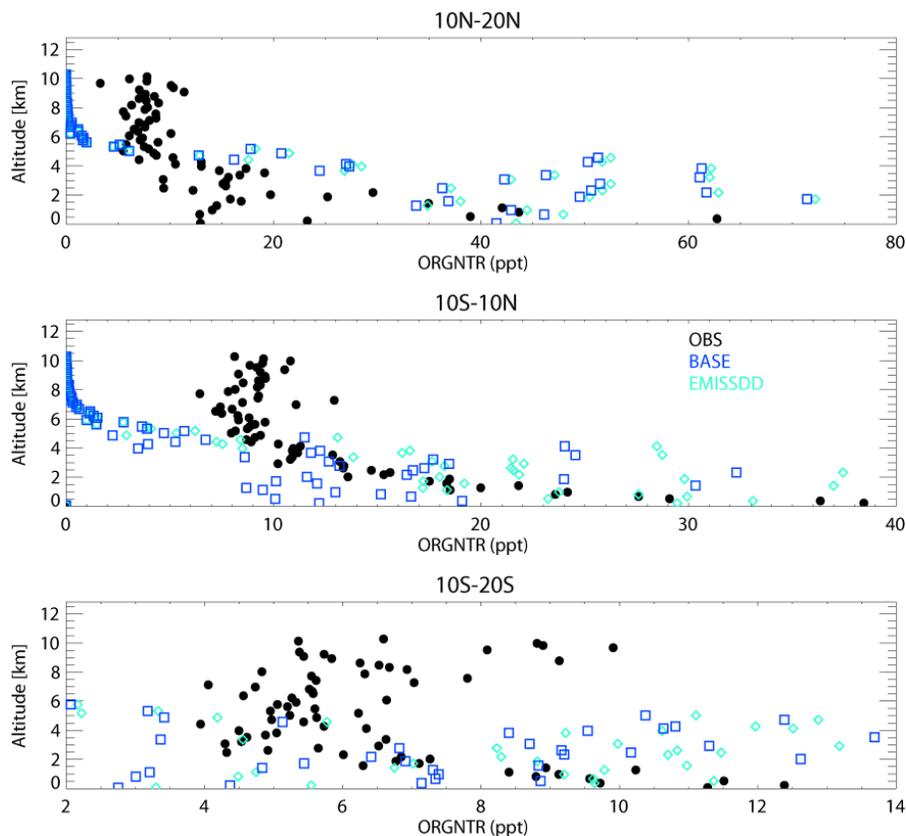
Fig. 7. A comparison of the distribution of higher alkyl nitrates as measured during March in the PEM-Tropics B measurement campaign and that simulated in the TM5 global CTM. The simulations shown are for BASE (blue) and EMISS (orange).
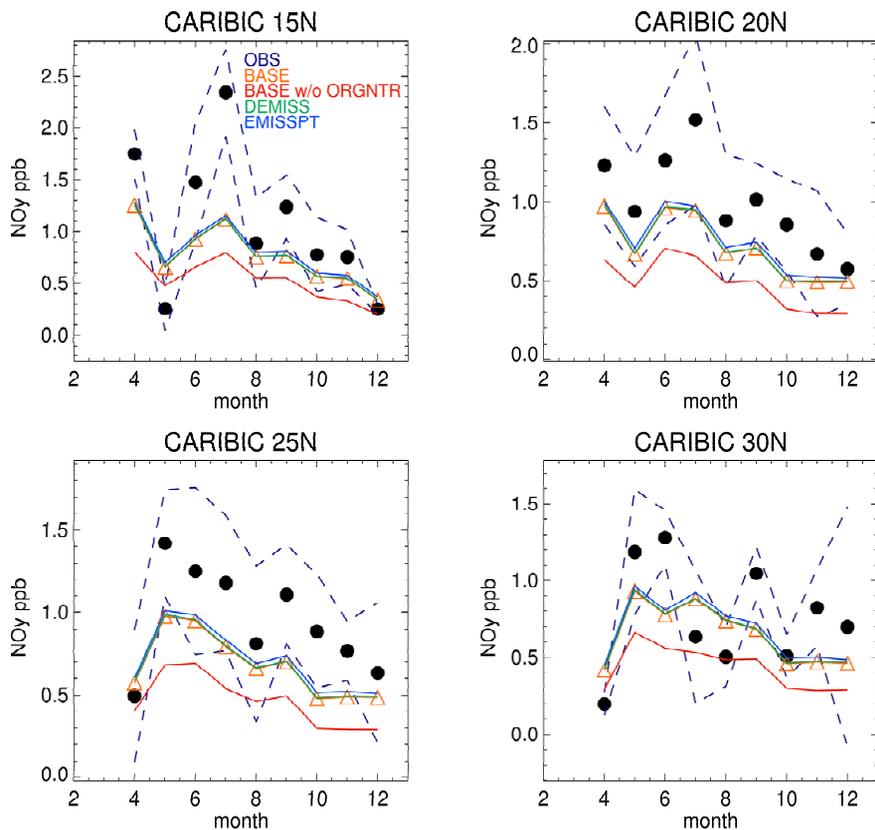
Fig. 8. A comparison of CARIBIC NO_y measurement data (black) sampled in selected latitudinal bins with corresponding model output for the BASE (yellow triangles), DEMISS (green) and EMISSPT (blue). Also show is BASE NO_y without the contribution from alkyl nitrates (red). The 1-σ variability in the observations is indicated by the dashed blue line.
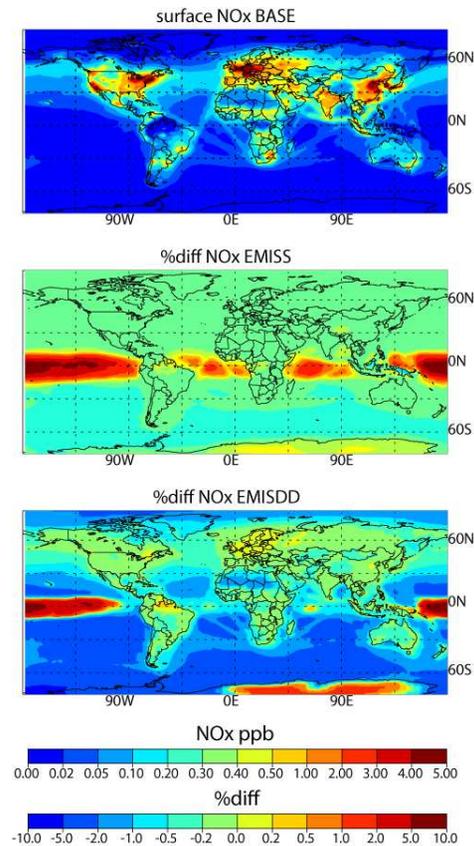
Fig. 9a. The annual surface distribution of NO_x integrated below 800 hPa (top), along with the percentage differences introduced in the EMISS (middle) and EMISSDD (bottom) simulations with TM5. The percentage differences are calculated according to $(BASE - SENS / BASE) \cdot 100$. In TM5 NO_x is defined as the sum of NO, NO_2, NO_3, HNO_4 and N_2O_5
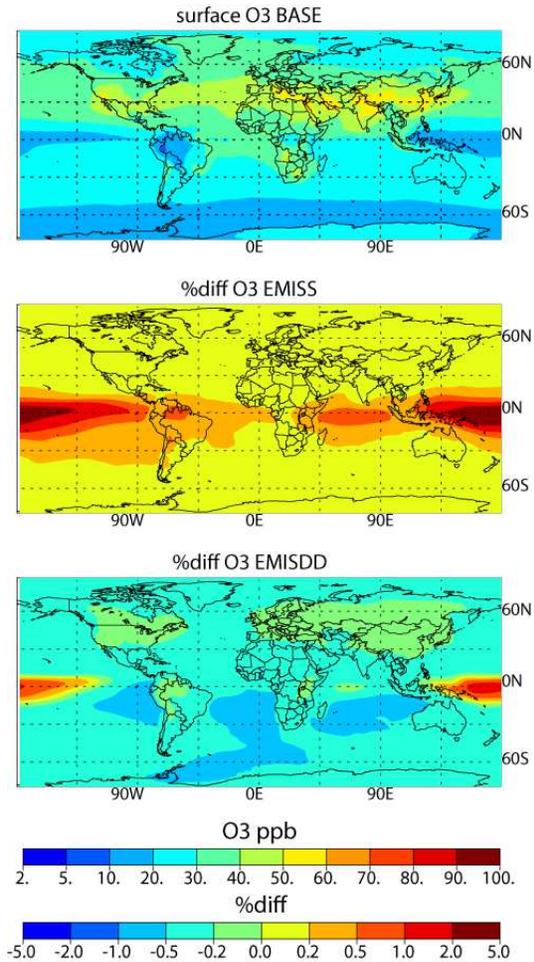
Fig. 9b. As for Fig. 9a except for tropospheric ozone.

Title Page

Abstract | Introduction

Conclusions | References

Tables | Figures

◄ | ►

◄ | ►

Back | Close

Full Screen / Esc

Printer-friendly Version

Interactive Discussion
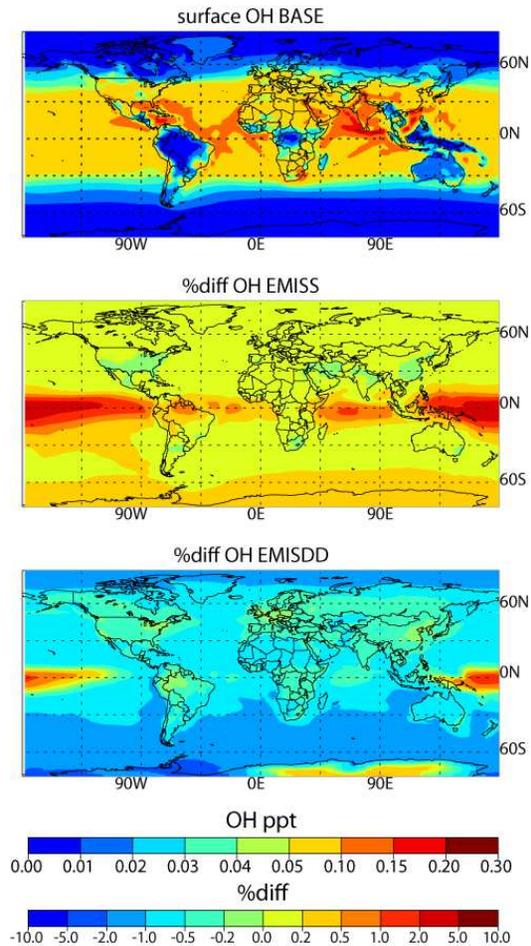
Fig. 9c. As for Fig. 9a except for tropospheric OH.

Title Page

Abstract | Introduction

Conclusions | References

Tables | Figures

|◀ | ▶|

◀ | ▶

Back | Close

Full Screen / Esc

Printer-friendly Version

Interactive Discussion